

Catalysts

for Environment, Energy and Health

Prof. IN, SU-IL

Dept. of Energy Science & Engineering

DGIST



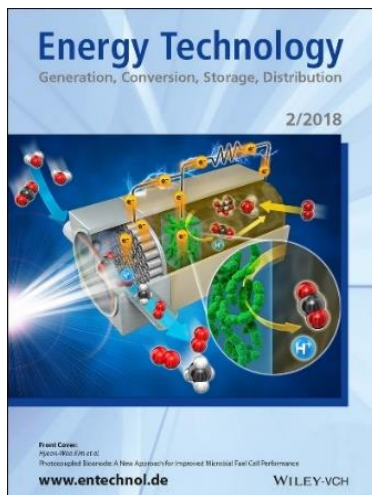
DGIST,
WHERE THE
CONVERGENCE
BEGINS

DGIST is a research-oriented university with a full support from Korean government.

DGIST started with a research institution in 2004 and grew into a research-oriented university by opening graduate program in 2011, and the undergraduate program in March, 2014. DGIST focuses its research and education in six areas, such as Emerging Materials Science, Information & Communication Engineering, Robotics Engineering, Energy Science and Engineering, Brain Science, and New Biology.



Microbial Fuel Cell for H₂



Photocoupled Bioanode: A New Approach for Improved Microbial Fuel Cell Performance

Energy Technology, 6(2), 2017



Nuclear Power Battery



C-14 Powered Dye-Sensitized Betavoltaic Cells

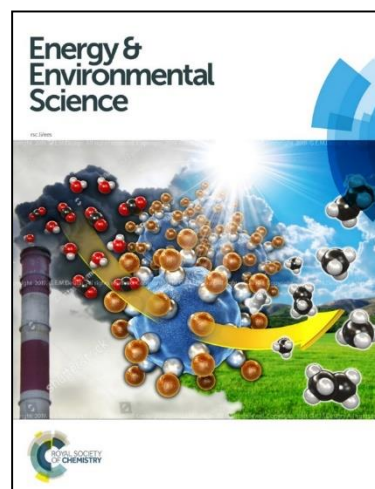
Chemical Communications (2020) 56, 7080-7083

CO₂ Utilization



CO₂, Water, and Sunlight to Hydrocarbon Fuels: A Sustained Sunlight to Fuel (Joule-to-Joule) Photoconversion Efficiency of 1%

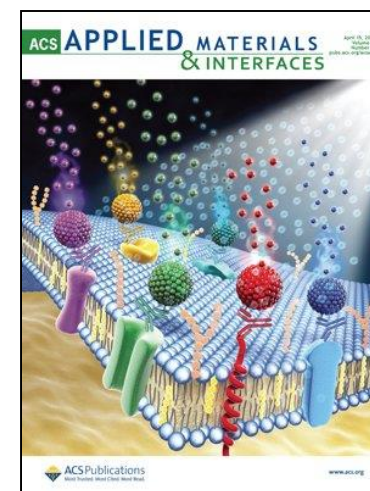
Energy & Environ. Sci. (2019) 12, 2685 - 2696



High-Rate Solar-light Photoconversion of CO₂ to Fuel : Controllable Transformation from C₁ to C₂ Products

Energy Environ. Sci., 11 (2018) 3183 - 319

Nano-Bio Hybrid Technology



Multiplex Protein Imaging with Secondary Ion Mass Spectrometry Using Metal Oxide Nanoparticle Conjugated Antibodies

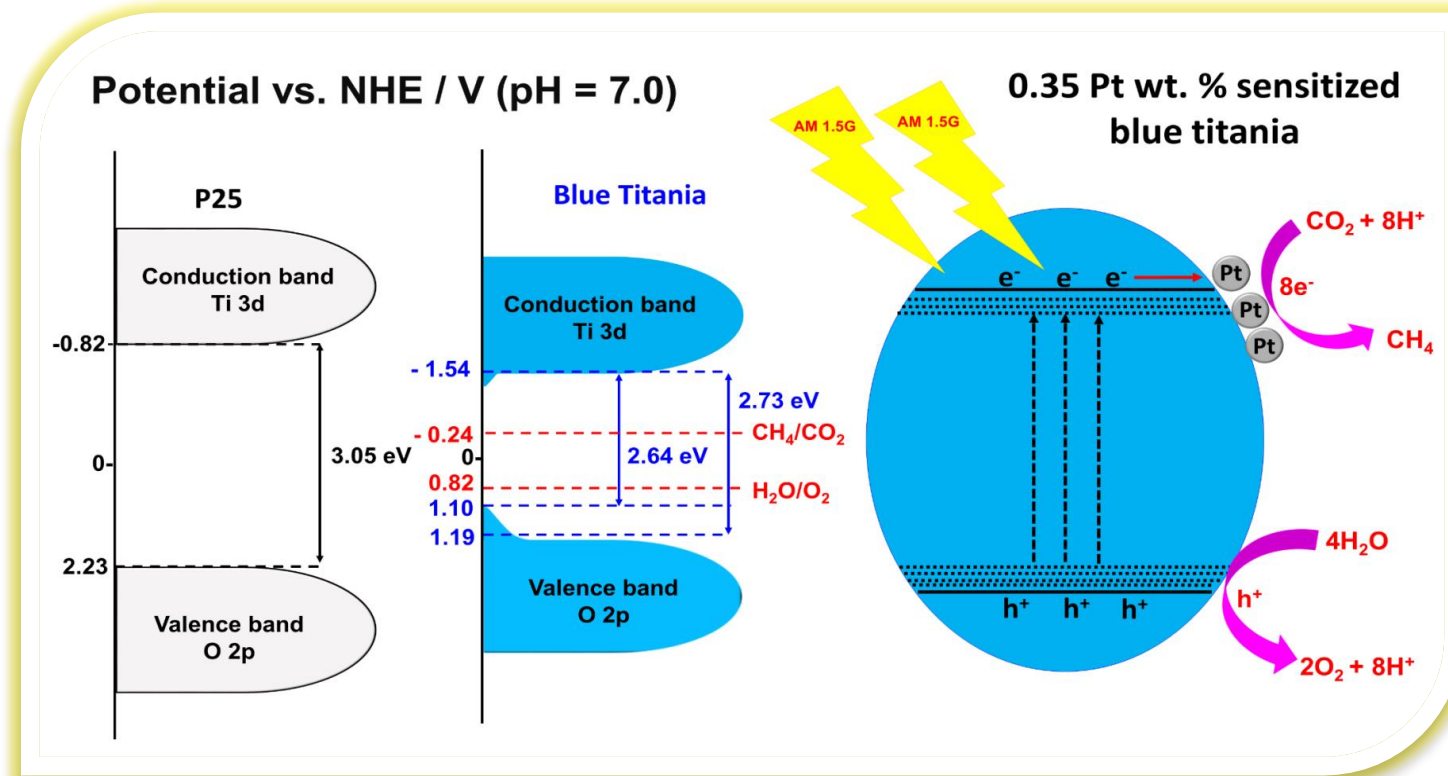
ACS Applied Materials and Interfaces (2020) 12, 18056-18064



Enhanced Therapeutic Treatment of Colorectal Cancer Using Surface-Modified Nanoporous Acupuncture Needles

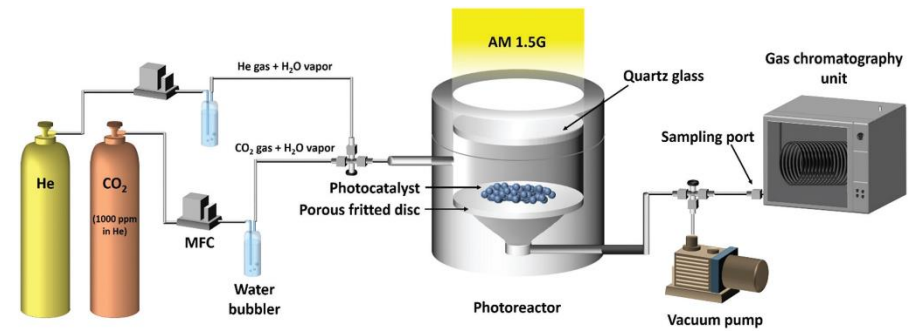
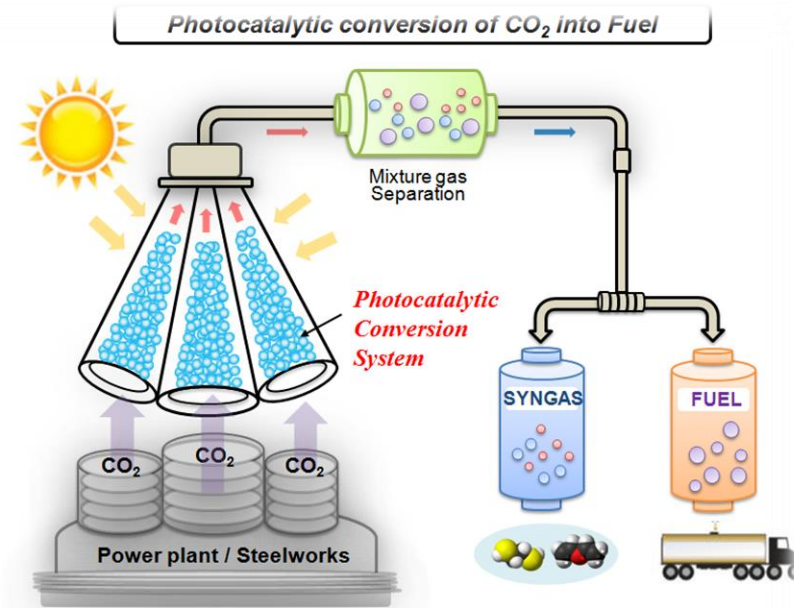
Scientific Reports 7 12900 (2017)

Topic 1 : Solar Light Driven CO₂ Reduction into Fuels



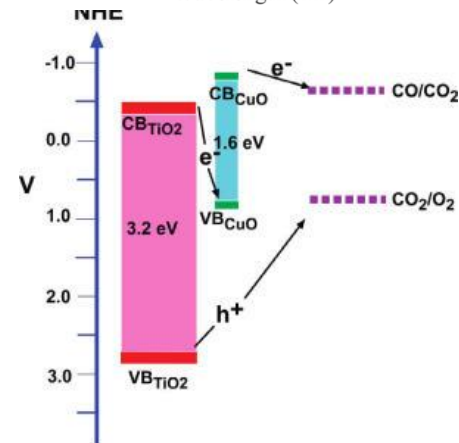
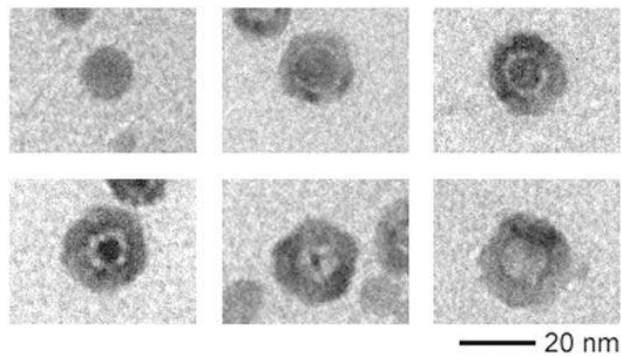
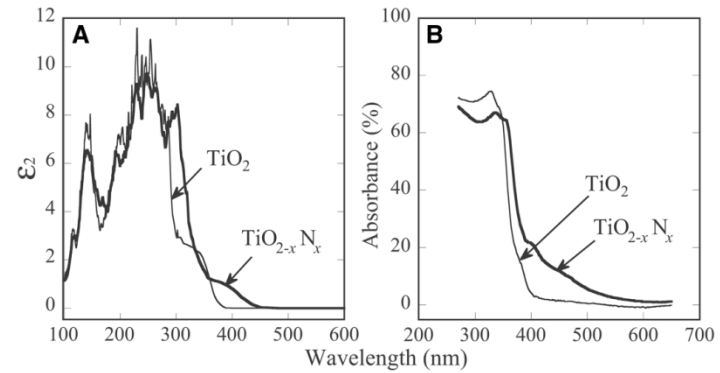
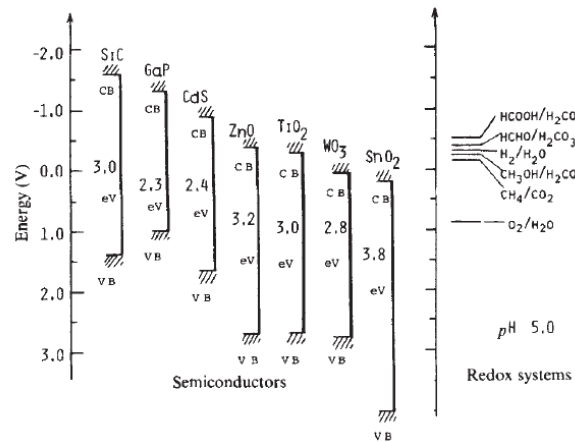
- *Materials Today* (2017) 20, Issue 9, 507-515
- *Applied Catal. B* (2017) 215, 28-35
- *Energy Environ. Sci.* (2018) 11, 3183 - 319
- *Energy Environ. Sci.* (2019) 12, 2685 - 2696
- *Applied Catal. B* (2020) 279, 119344
- *Chem. Eng. J.* (2020) in press

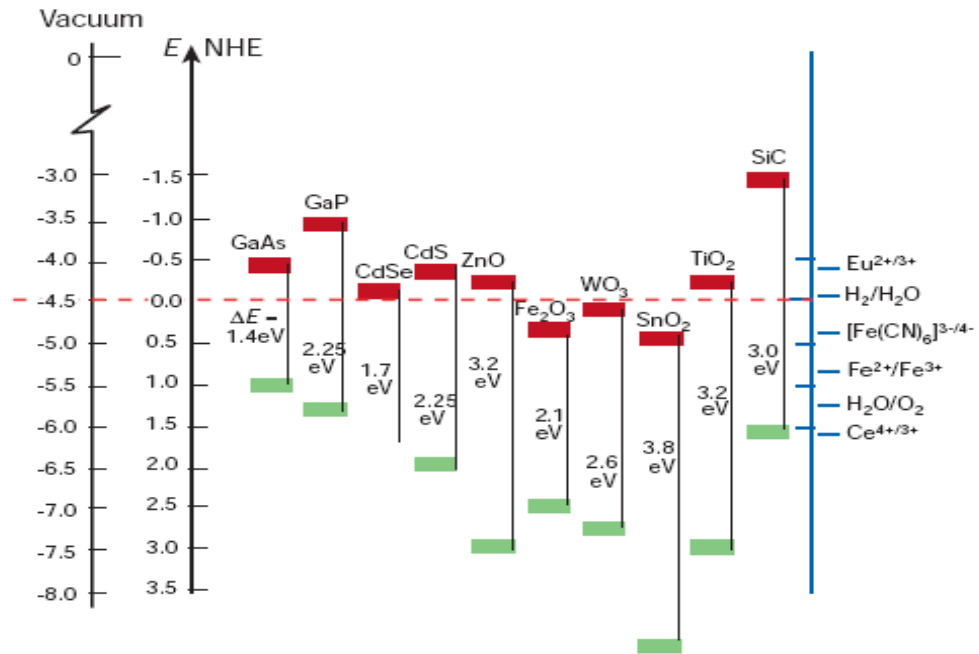
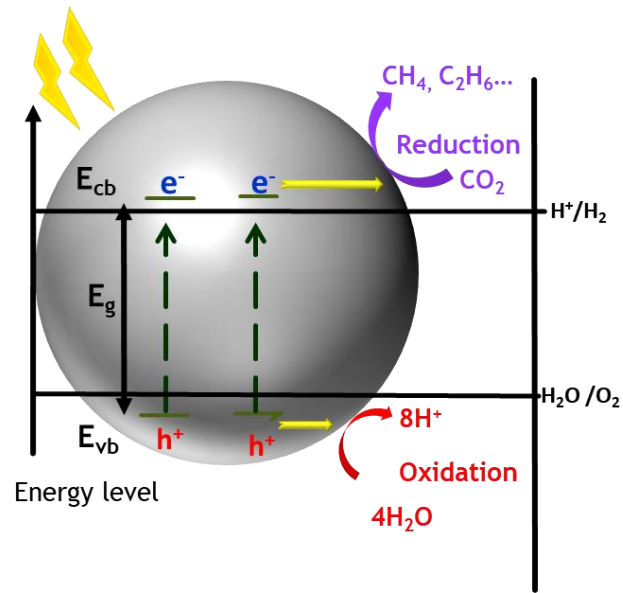
CO₂ Conversion into Fuels ?!



Nano material synthesis for green energy application

- CO₂ conversion into organic compounds, K. Honda et al., *Nature* 1979, 277, 637-638.
- Visible light photocatalysis in N-doped TiO₂, R. Asahi et al., *Science*, 2001, 293, 269-271.
- Formation of hollow nanocrystals, P. Alivisatos et al., *Science* 2004, 304, 711-714.
- Ideal combination for CO₂ conversion, C. Grimes et al., *ACS NANO*, 2010, 4, 1259-1278.





Bulk and nanoscale inorganic materials

Nanofabrication techniques

Coating techniques (thin-film)...CVD, PVD, electrochemical deposition, sputtering

Bandgap engineering:

doping/cocatalysts/sensitizer/quantum dot

Pt, Au, Cu, NiO...

TiO₂ as a reference and standard material:

non-toxicity, high photoactivity, mechanical stability, low cost,

favorable overlap with the UV portion of the solar spectrum

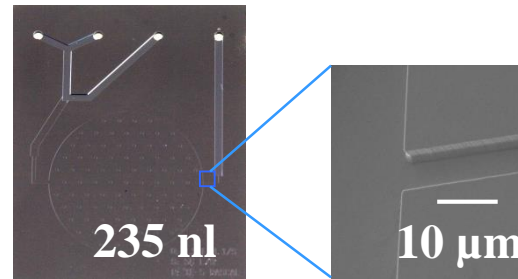
Reactor Design for Photocatalytic Gas Phase Reaction



114 ml

2004~2008

Chem. Comm. 40 (2006) 4236 - 4238
 JACS 129 (45) (2007) 13790-13791
 Energy & Environ. Sci. 2(12) (2009)1277-1279.

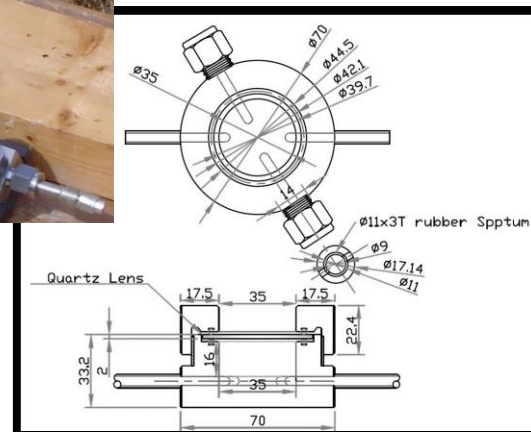


2009~2010

JPC C, 2010, 114 (25), 11162-11168
 Chem. Comm. 2011, 47 (9), 2613 - 2615
 J Photochem. Photobio. A 2011, 222(1), 258-262
 J Catalysis, 2012, 289, 62-72



2011 ~ 2012



2012 ~

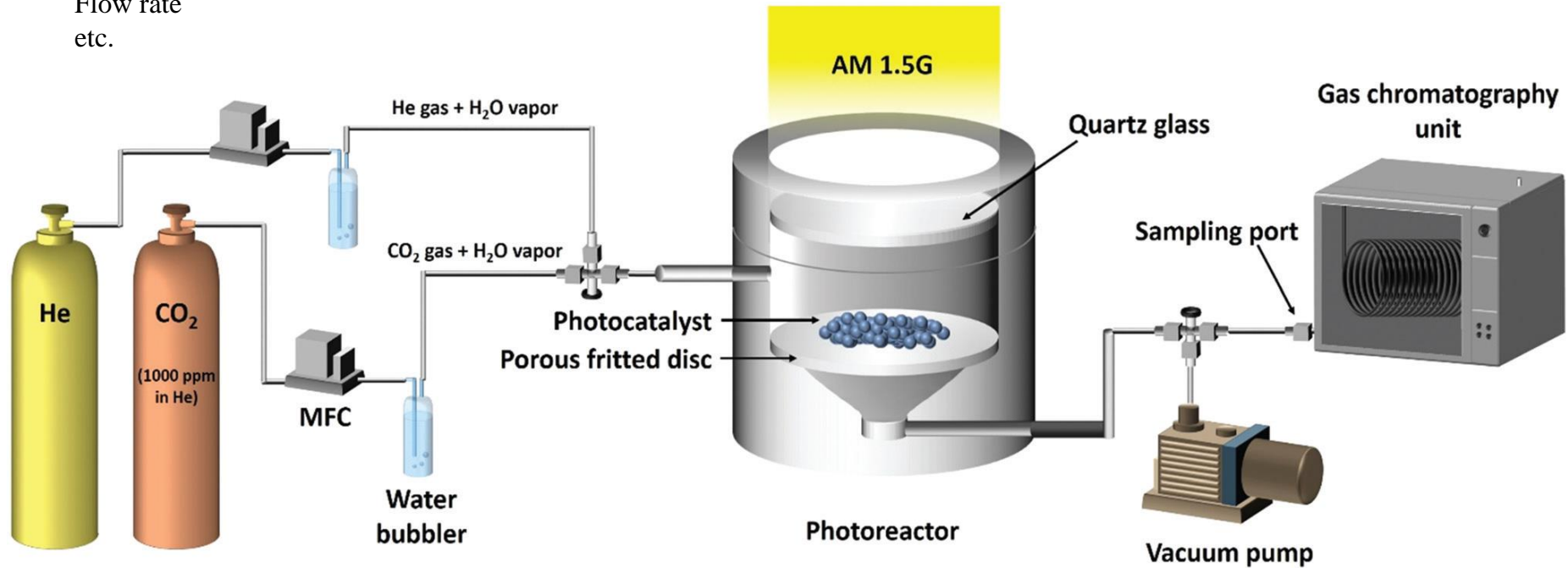


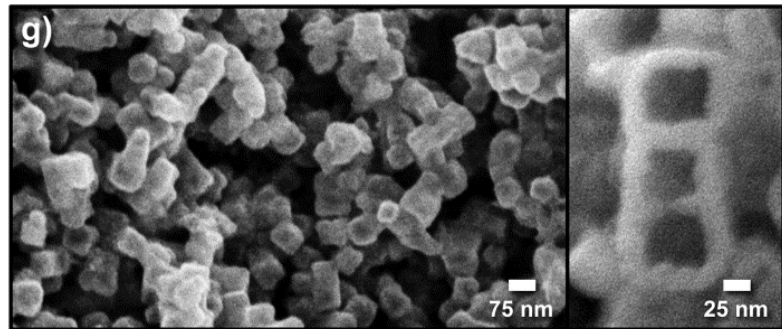
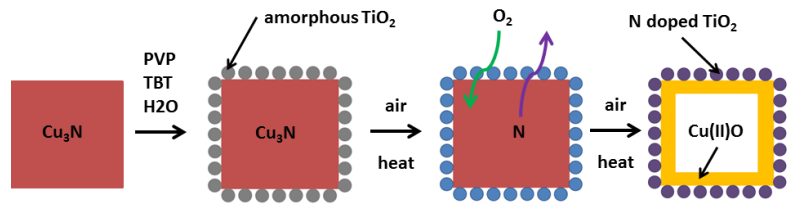
Solar-thermal reactor

Angew. Chem. Inter. Ed. 51 (2012) 3915- 3918
 Rapid Comm. Photosci. 2013, 2 (2), 64-66
 ACS Omega, (2016) 1, 868-875
 Carbon 98 (2016) 537-544.
 Journal of CO2 Utilization 20 (2017) 301-311

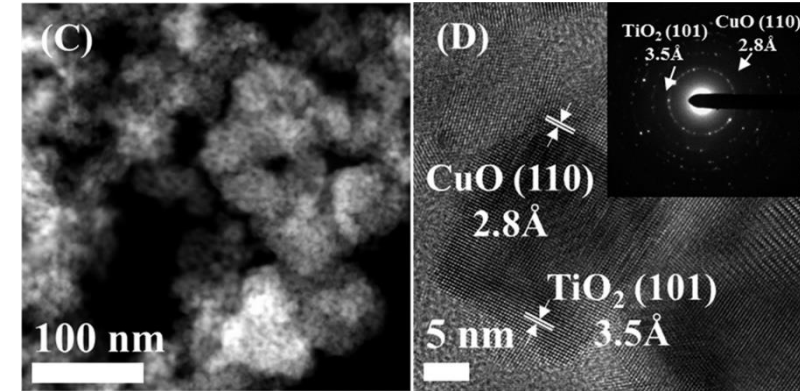
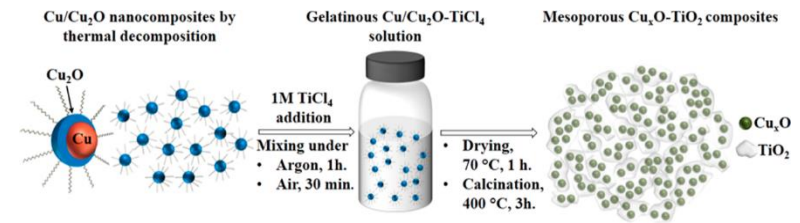
Gas Phase Flow Reactor System

Residence time
Geometry
Dead volume
Leak control
Pressure
Flow rate
etc.

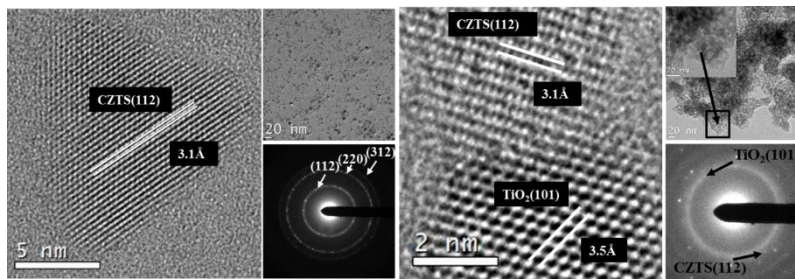
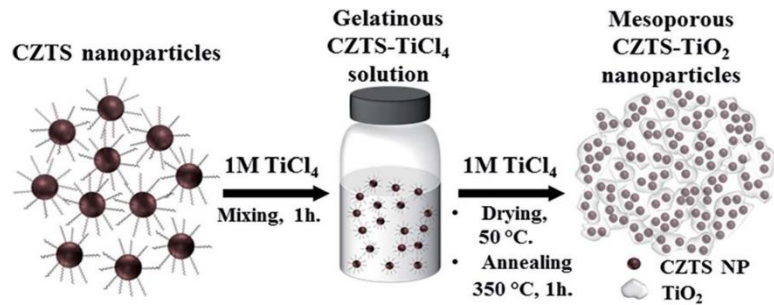




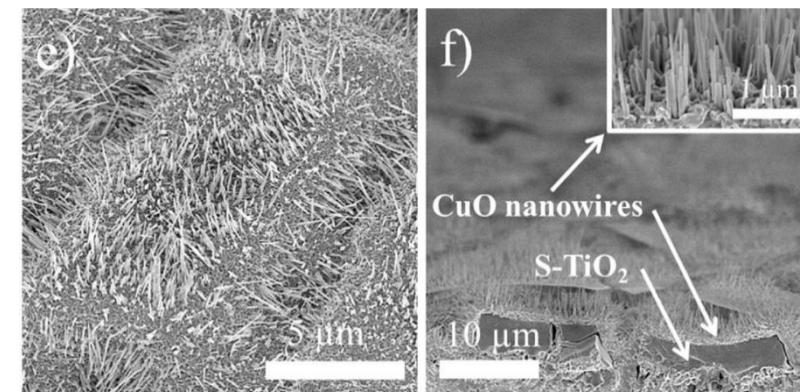
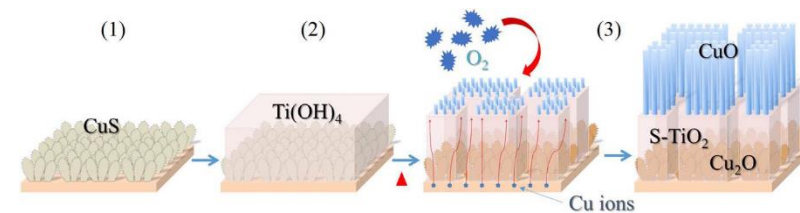
Angew. Chem. Int. Ed. 51 (2012) 3915- 3918



ACS Omega 1 (2016) 868–875



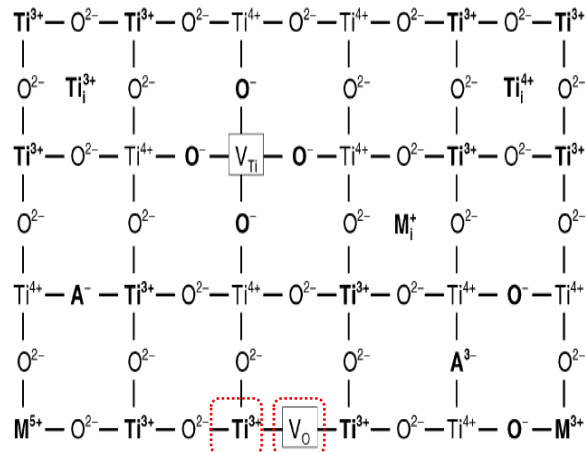
RSC Adv., 2016, 6, 38964–38971



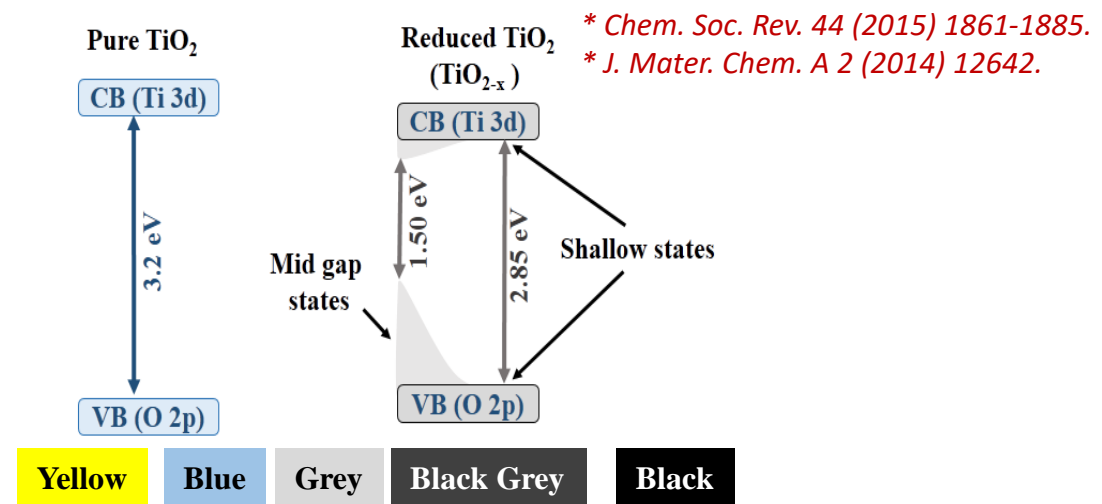
J. of CO₂ Utilization 20 (2017) 91–96

Distinct Features of Reduced Titania

- Surface defects, oxygen vacancies (V_O) and Ti^{3+} ions:
 - Responsible for new shallow or deep mid gap energy states
 - Also acts as electron/hole traps rather than a recombination center



* *J. Phys. Chem. C. 112 (2008) 5275-5300.*



Interaction with CO_2

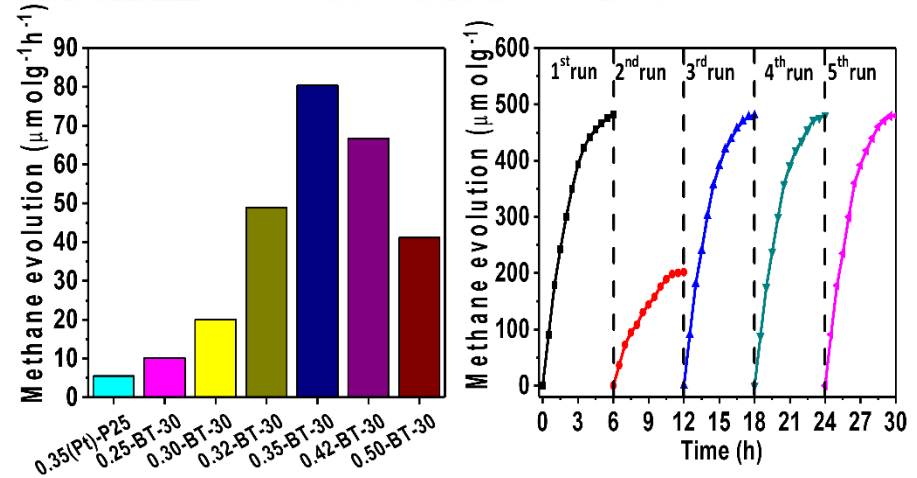
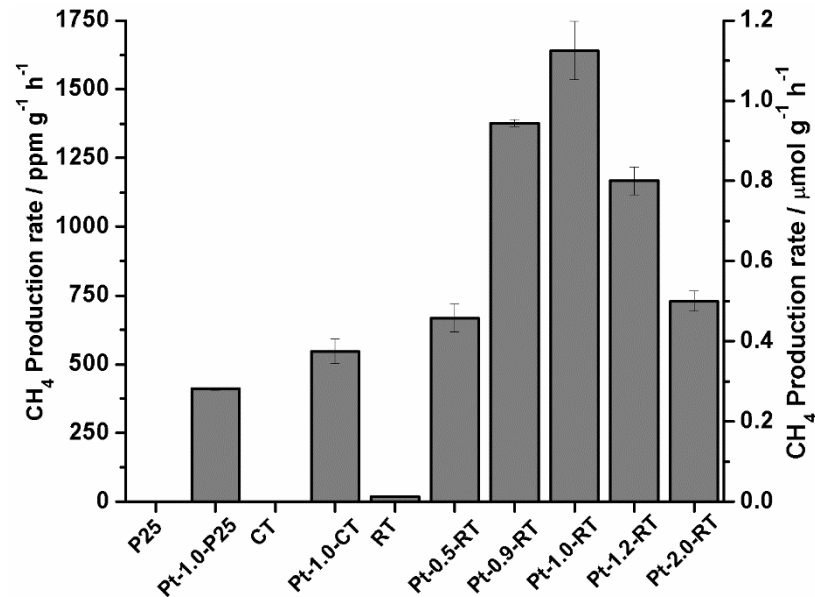
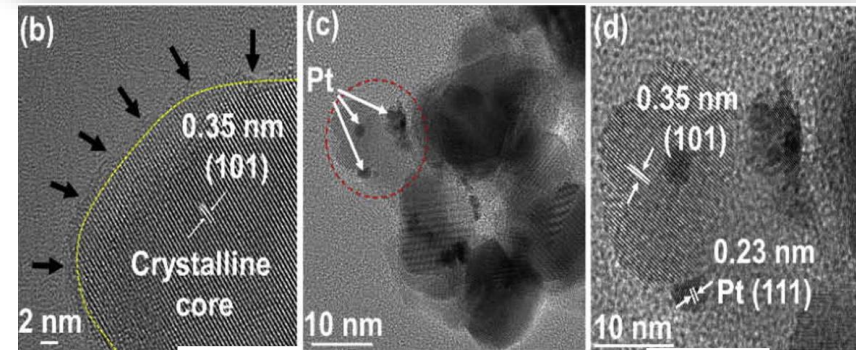
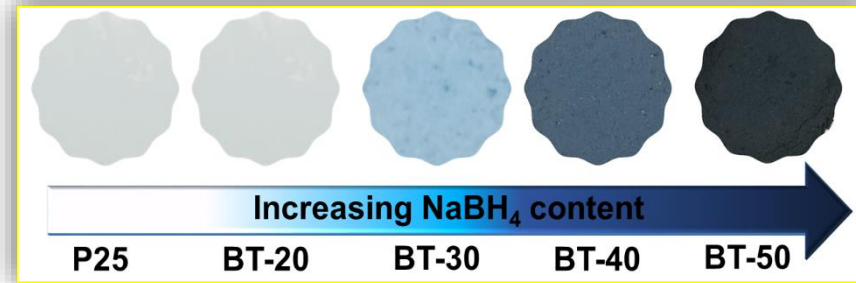
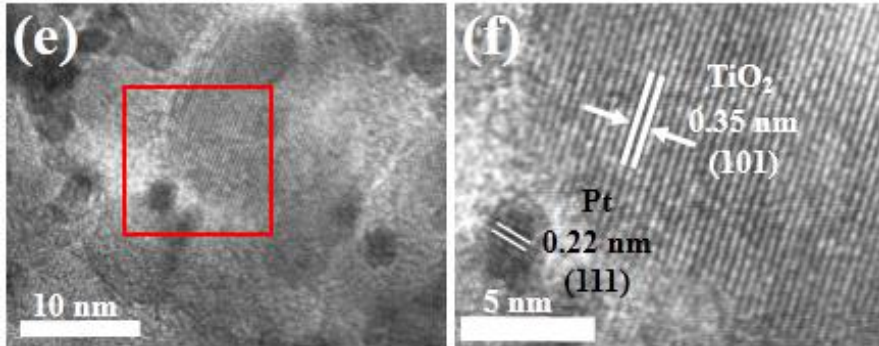
- Oxygen vacancies (V_O) offer **chemical adsorption sites for CO_2**
- V_O favours the dissociation of CO_2 on the surface of TiO_2
- **Oxygen deficient surfaces are more thermodynamically favourable to adsorb CO_2** than defect-free surfaces

Interaction with H_2O

- Defect sites **promote the adsorption and dissociation of water** on the surface of TiO_2
- Under illumination and in the presence of CO_2 and H_2O vapour, **more bridged HCO_3^- and $HCOOH$ species were formed on defective TiO_2** than on defect-free TiO_2 , according to an in situ DRIFTS study



- Annealed (650 °C, 4 h)
- HCl washed



Optimization of defects, band gap, band position

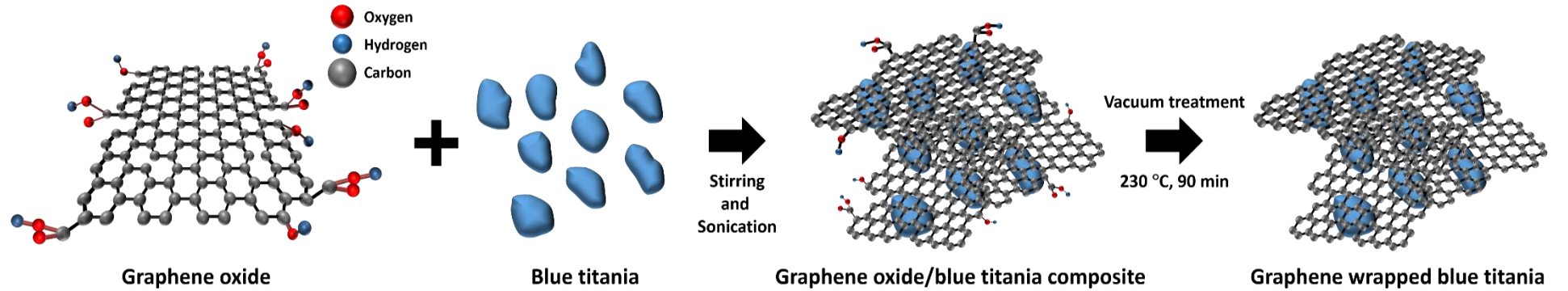
CH₄ yield of 80.35 μmol g⁻¹ h⁻¹ / 30 h stability

Materials Today 20 (2017) 507-515

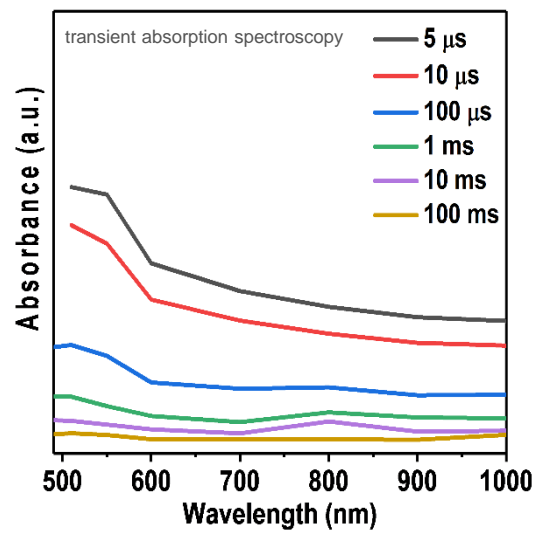
Applied Catalysis B 215 (2017) 28-35

High-Rate Solar-light Photoconversion of CO₂ to Fuel : Controllable Transformation from C₁ to C₂ Products

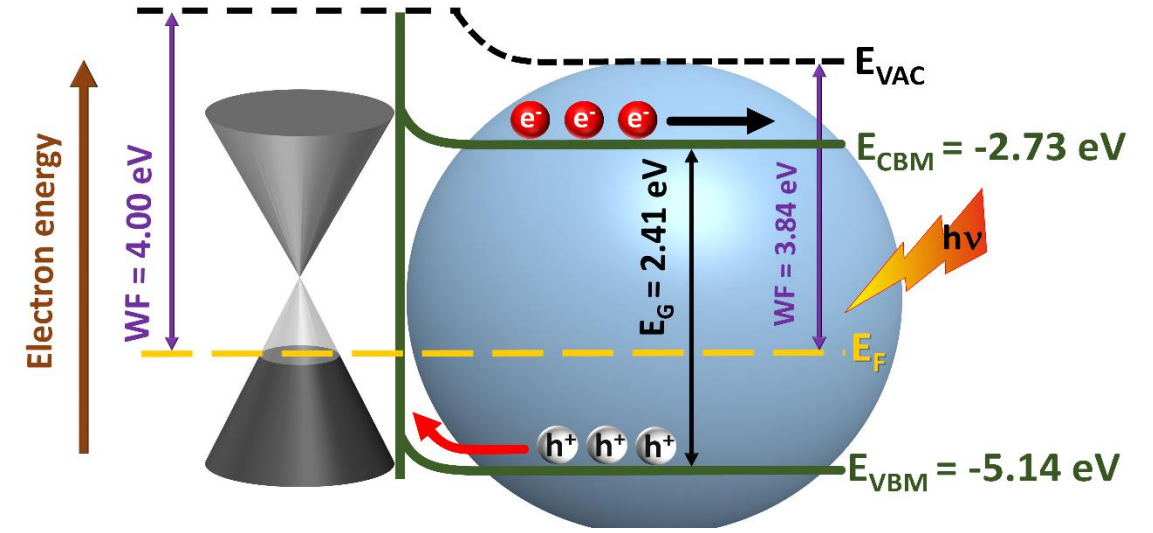
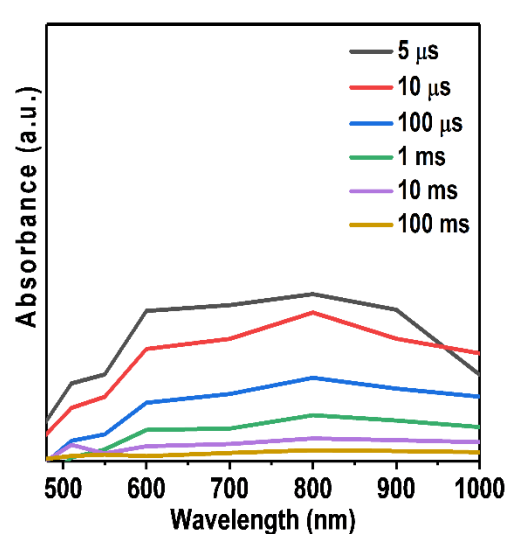
Energy Environ. Sci., 11 (2018) 3183 - 319



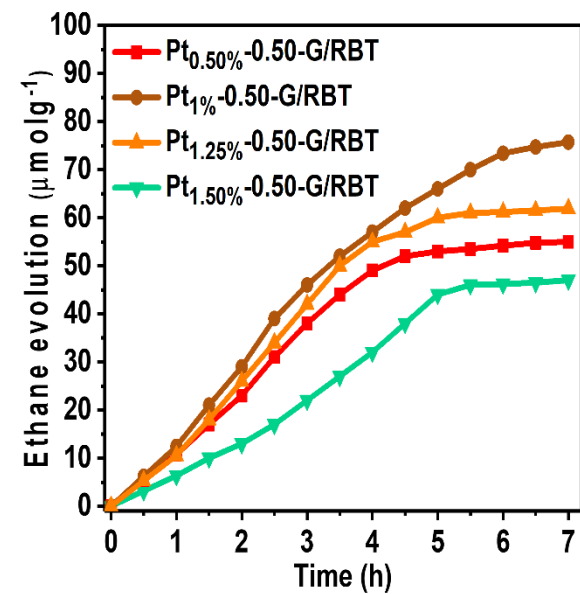
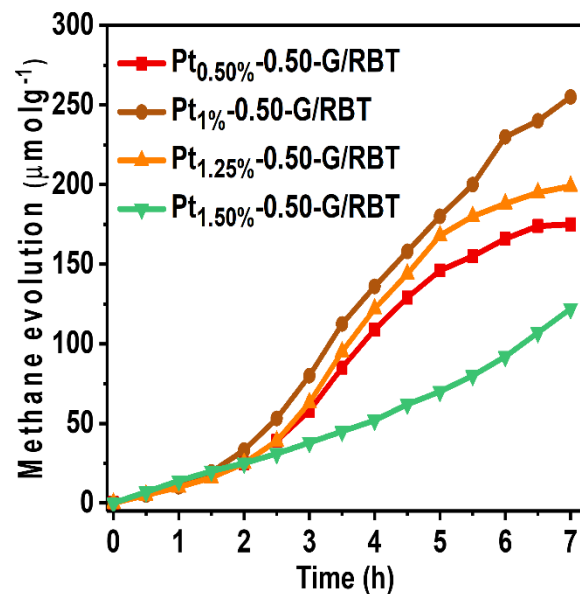
(TAS analysis) Hole and Electron signals in RBT



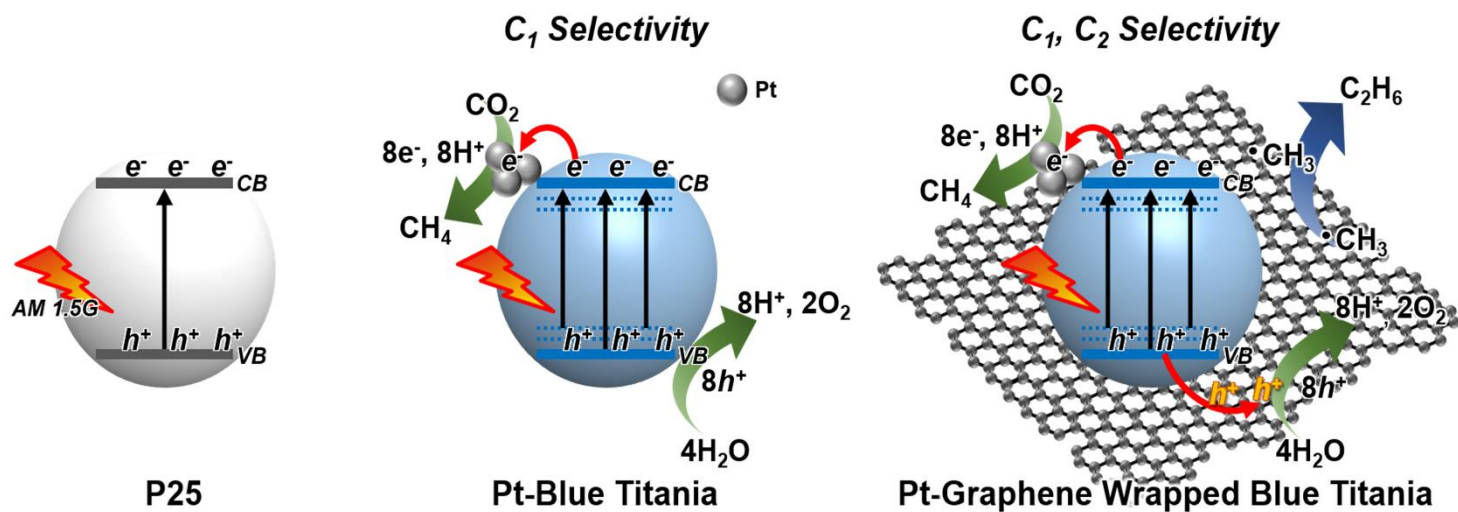
Quenched hole signal (510 nm) in 0.50G-RBT

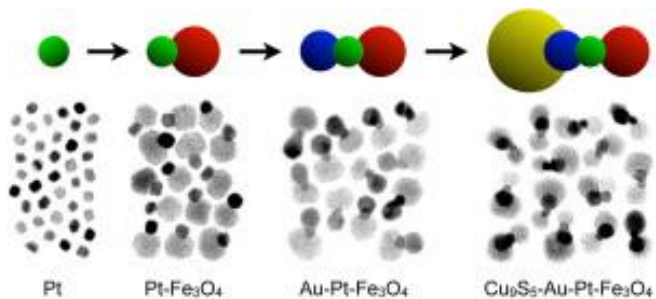


Photocatalytic CO₂ reduction results

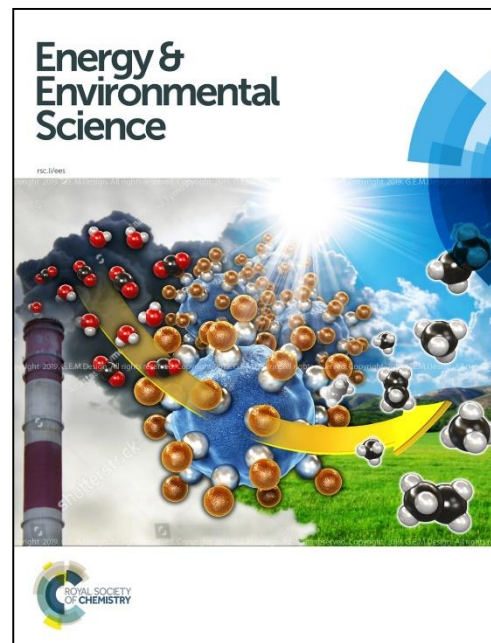


Transformation from C₁ to C₂ Products





R.E. Schaak et al., "A total synthesis framework for the construction of high-order colloidal hybrid nanoparticles," *Nature Chemistry* 2012, 4, 37-44.



**CO₂, Water, and Sunlight to Hydrocarbon Fuels:
A Sustained Sunlight to Fuel (Joule-to-Joule)
Photoconversion Efficiency of 1%**
Energy & Environmental Science (2019) 12, 2685 - 2696

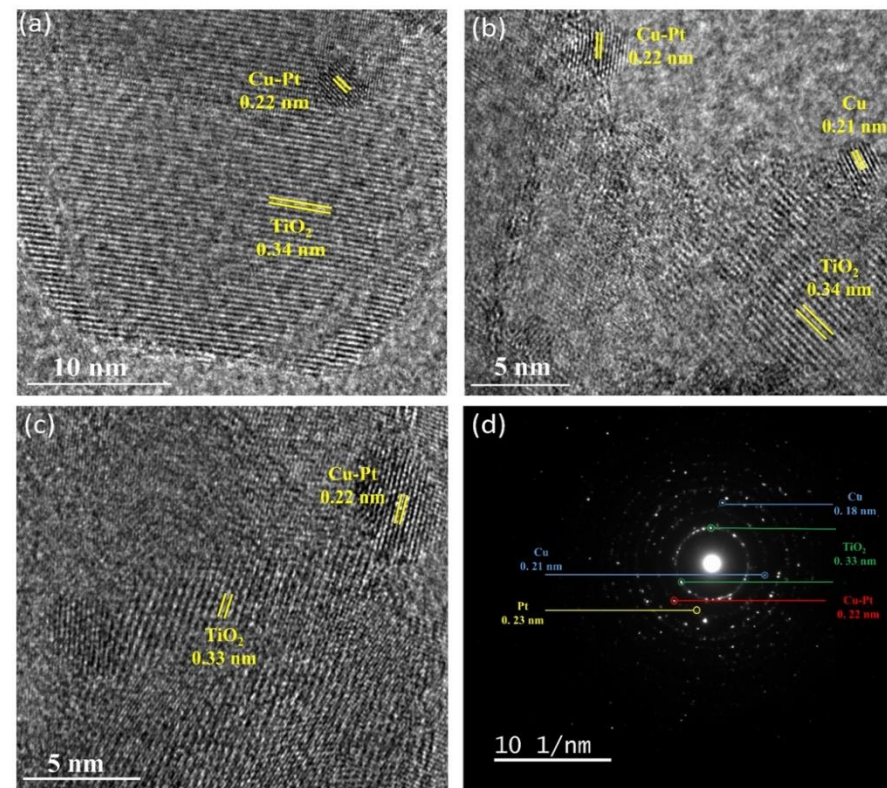


Figure 1: HR-TEM image of Cu_{1.00%}-Pt_{0.35%}-BT (inset showing SAED pattern of region encircled with yellow)

- ❖ The presence of **Pt and Cu-Pt alloys** is confirmed from the d-spacing of the *lattice fringes*, which are **0.23 nm (111) for Pt** and **0.22 nm and 0.18 nm (111) for Cu-Pt**
- ❖ **XPS analysis also confirms** the presence of Cu-Pt nanoparticles

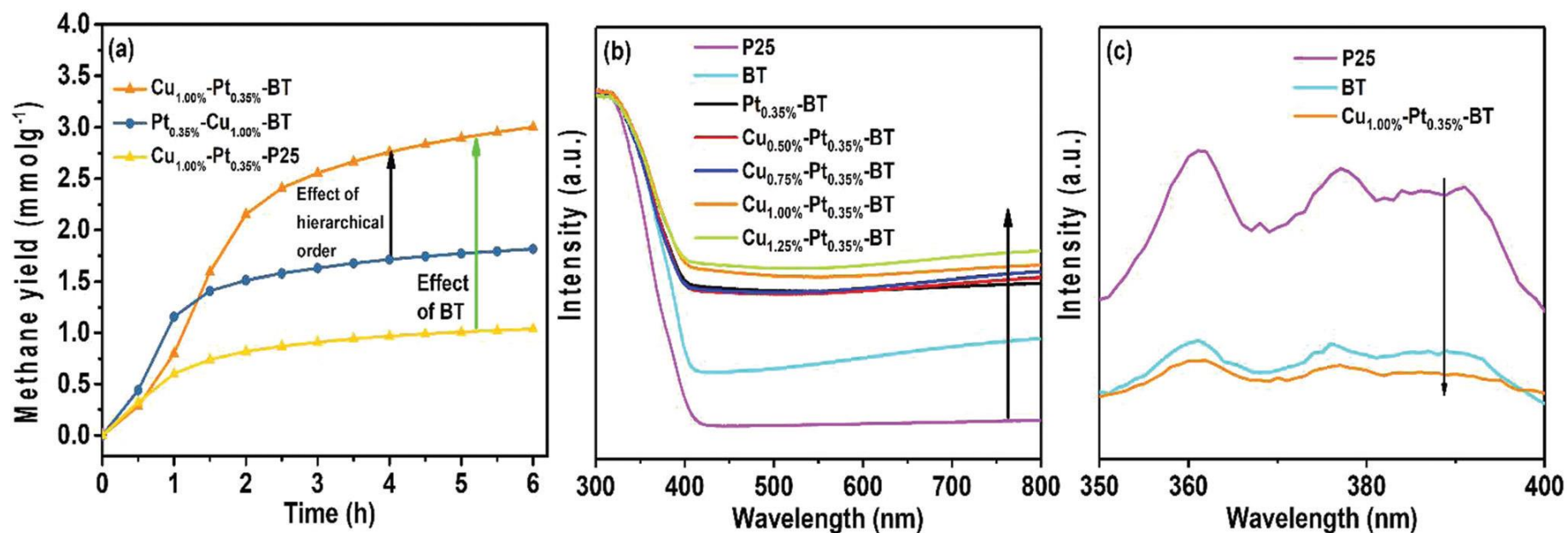
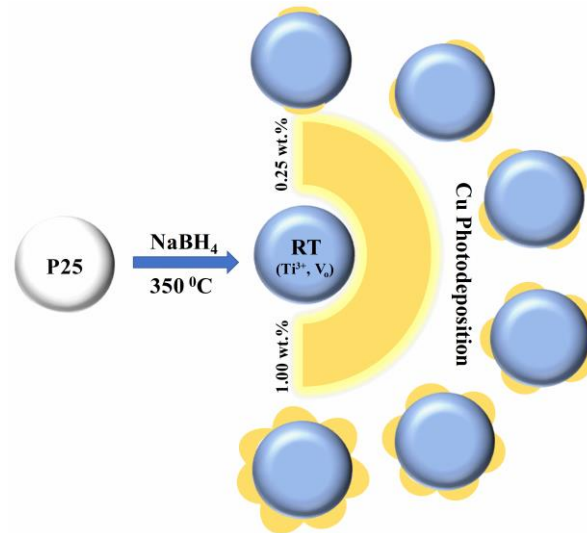


Fig. 2 Comparative methane evolution, UV-visible DRS, and PL spectra. (a) Effect of sample composition and structure on CO₂ photoconversion to CH₄ yield. (b) UV-visible diffuse reflectance spectra (DRS) indicate an enhancement in optical absorption with Cu–Pt nanoparticles, with absorption increasing with Cu content, and (c) PL spectroscopy indicates a better charge separation is observed for bimetallic deposited blue titania sample.

Cu₂O-reduced-titania (RT) Z-scheme Heterostructure

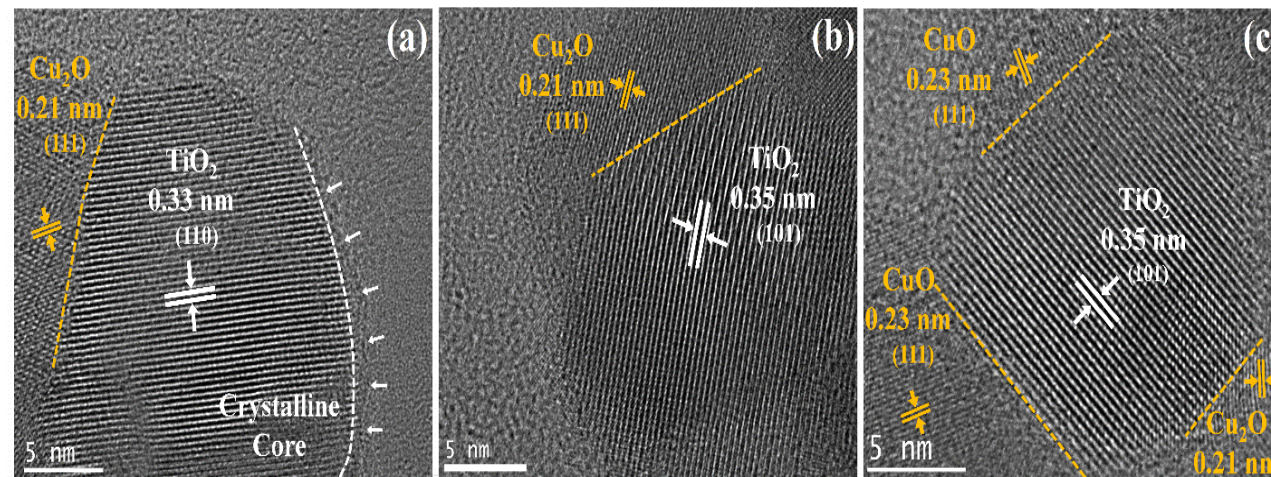
Synthesis Scheme



□ Why Cu₂O-RT heterostructure is unique????

- Interface is formed at electrons enriched defected core (white arrows fig(a)) as shown in the HR-TEM fig(a-c)
- Unlike core-shell structure, both catalyst can take part in the reaction
- Enriched electron density at interface avoids the Cu₂O oxidation

HR-TEM of RT-Cu₂O



Photocatalytic CO₂ Reduction over Cu₂O-RT Z-scheme

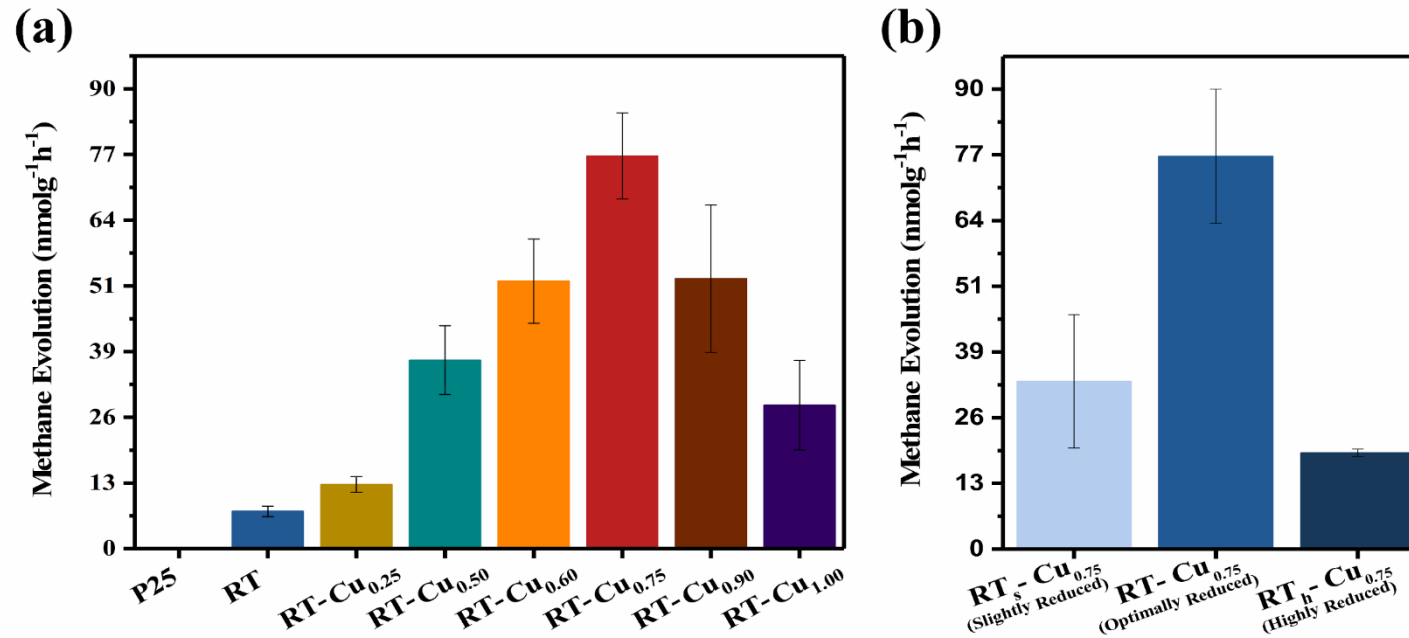
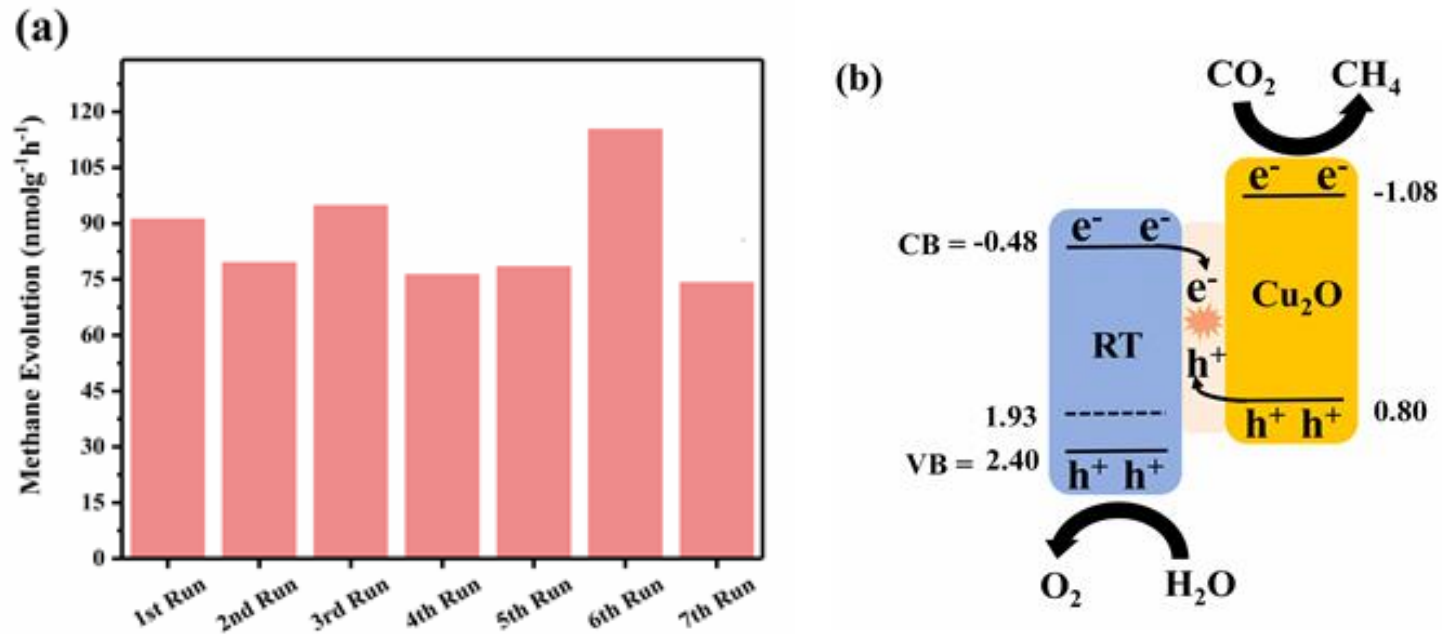


Fig. (a) Comparison of CH₄ evolution over a 6 h test for P25, RT, and RT-Cu_x; (b) CH₄ evolution for variable reduction degree from slightly reduced RTs-Cu_{0.75} to highly reduced RTh-Cu_{0.75}.

- Better charge separation, increased light harvesting and strong redox potential translated to 0.13% photoreduction of CO₂, **fig(a)**
- Optimum metal deposition (Cu = 0.75%) and defects (Ti³⁺, V_o) are essential for better performance, **fig(b)**

Synergistic effects of Cu₂O Z-scheme with RT, guarantee the efficient CO₂ photoreduction

Stability for Photocatalytic Reduction of CO₂



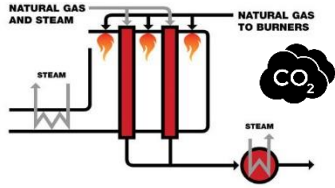
- Proposed stability is evident in CO₂ photo-reduction **fig(a)** for 7 cycles (total 42 h)
- Oxidizing h⁺ on Cu₂O are quenched by e⁻ from the RT as shown in **fig (b)**
- Amorphous interfacial layer ensures the supply of e⁻ to quench Cu₂O oxidizing h⁺

Charge transfer/separation and CO₂ reduction performance/stability confirms

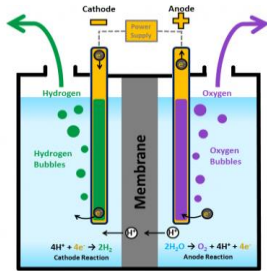
stable Z-scheme heterostructure of RT and Cu₂O

Topic 2: Hydrogen Production by Hybridization of Microbial Electrolysis Cell and photoanode

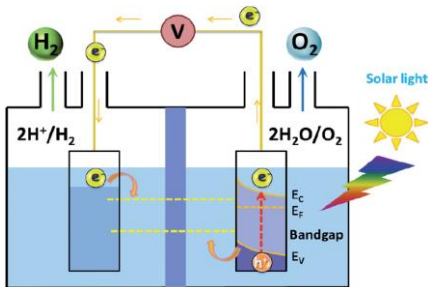
STEAM METHANE REFORMING



SMR

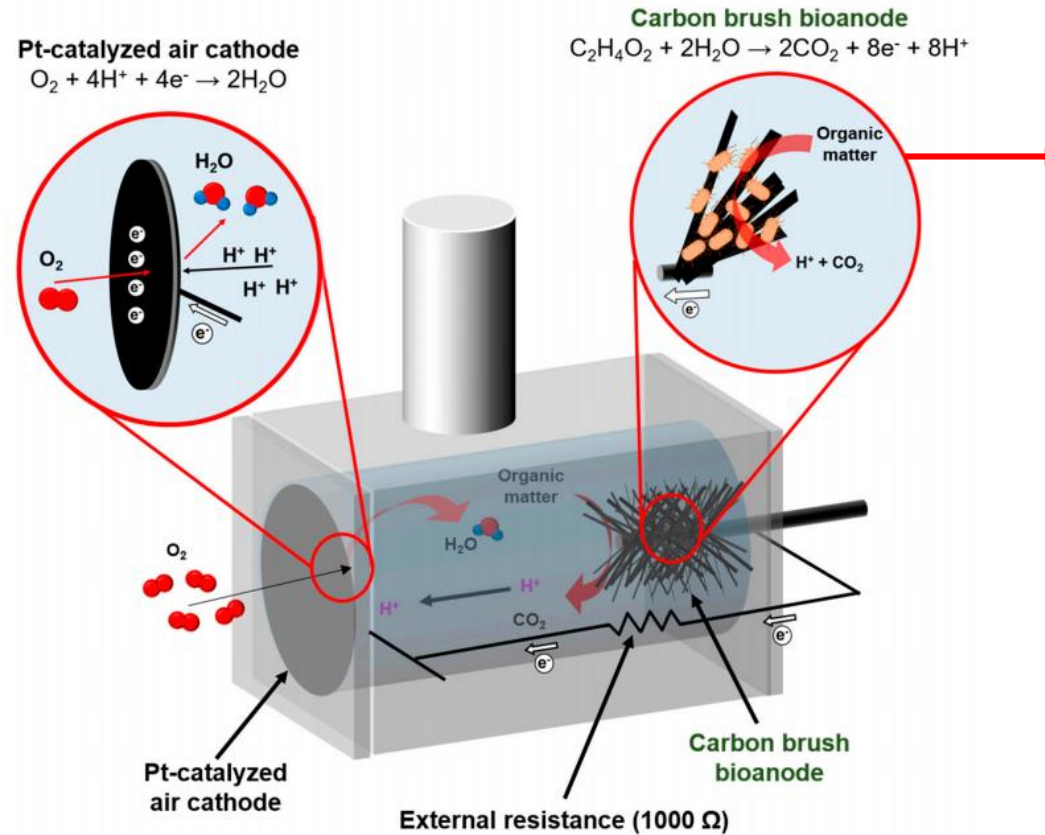


ECs



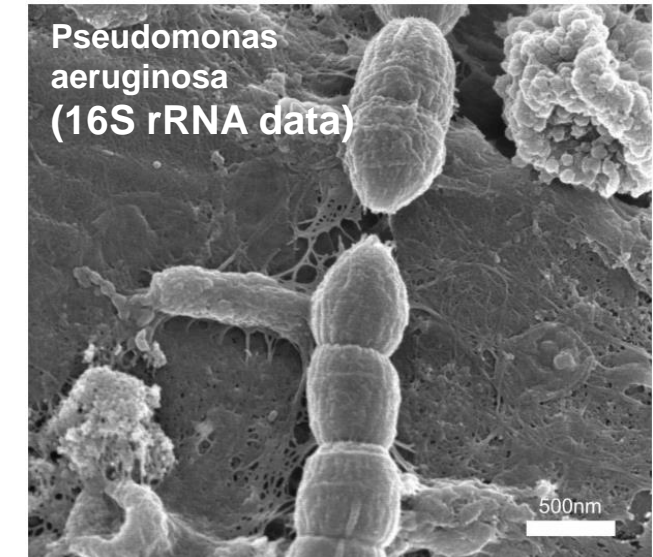
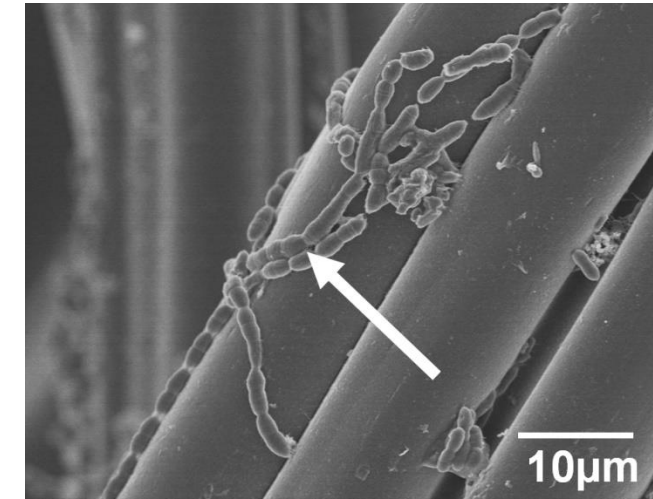
PECs

- Microbial Fuel cells (MFCs)



- MFCs produce electricity with decomposing organic matter (in wastewater).

Exoelectrogens



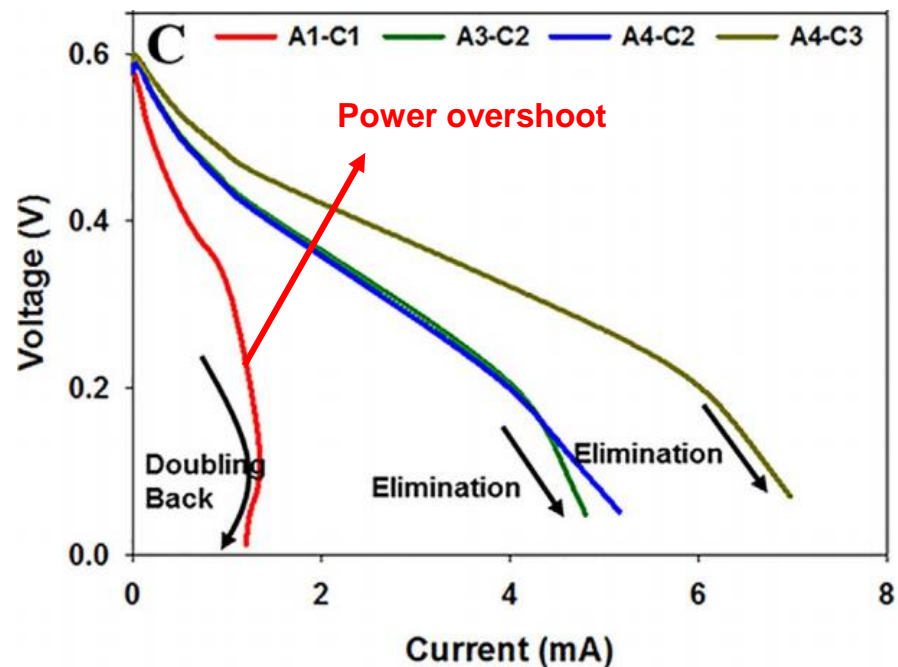
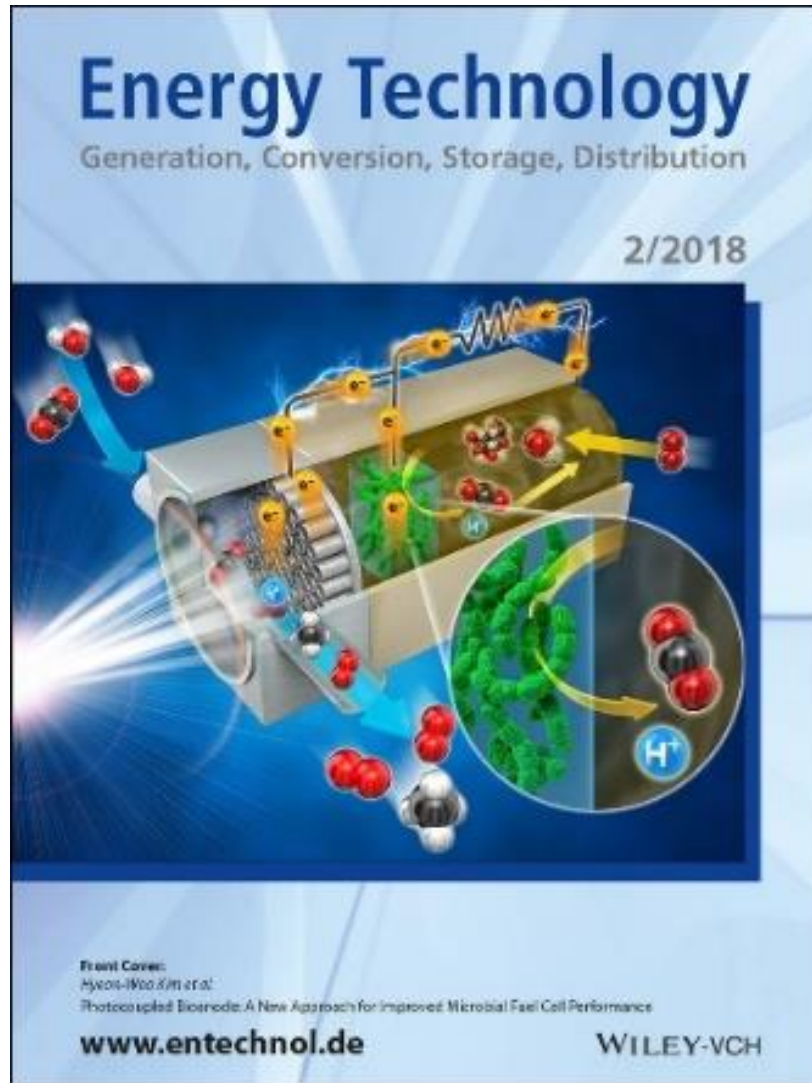


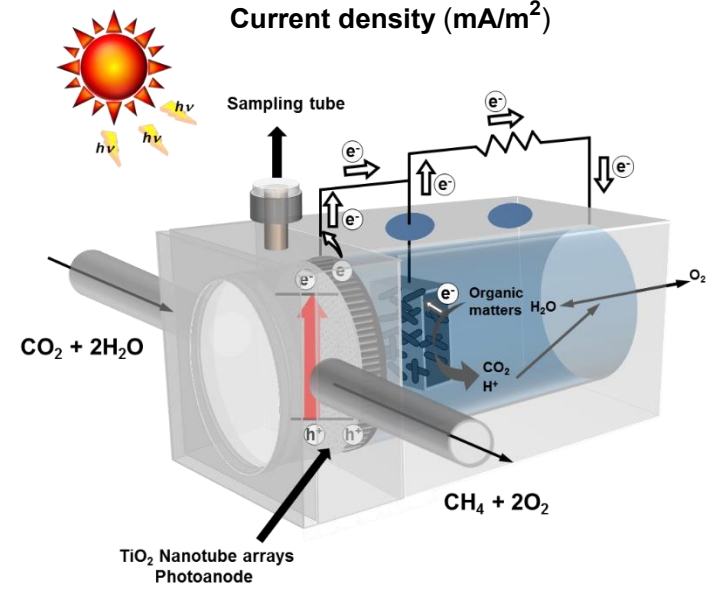
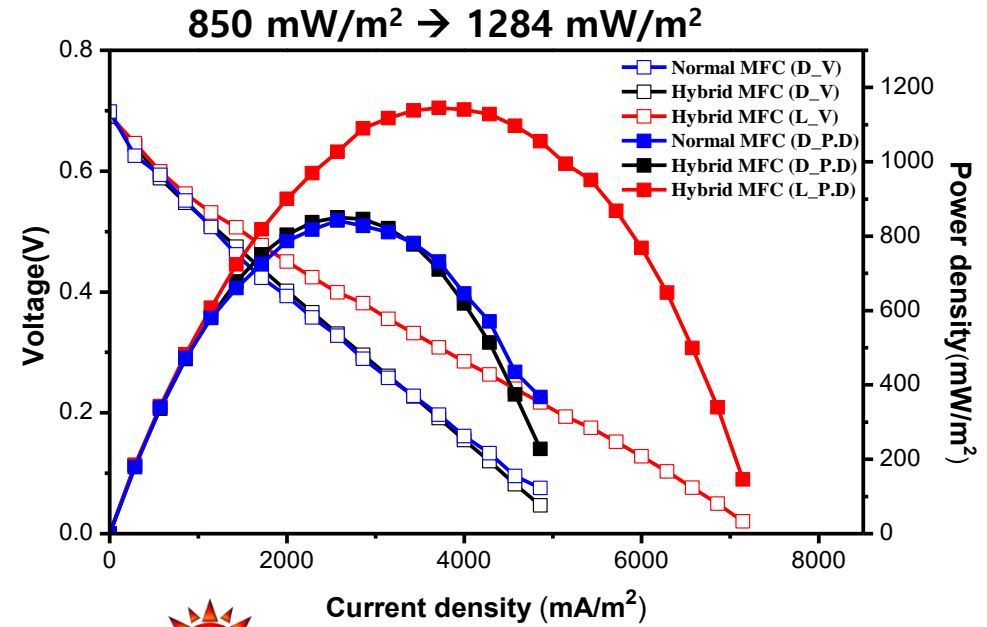
Fig 7. Power overshoot on MFCs

- The **power overshoot** is defined as a “doubling back” of the voltage and power curves toward lower currents, rather than increasing to the expected higher current.
- Ax-Cy: A means anodes and x is the number of anodes
C means cathodes and y is the number of cathodes (A3-C2, A4-C2, and A4-C3 MFC).
- Power overshoot is eliminated by using more anodes.

Table 1. Summary of causes of power overshoots in previous studies.		
Causes of power overshoot	Previous study	Ref.
Increase of internal resistance, ionic depletion	Ieropoulos et al., 2010	[9]
Increase of internal resistance	Liu et al., 2011	[10]
Inadequate scan time of discharge test, insufficient inoculation of bioanode, limited organic concentration	Winfield et al., 2011	[11]
Inadequate scan time of discharge test	Watson and Logan, 2011	[12]
Poor acclimation of microbes	Hong et al., 2011	[13]
Poor acclimation of microbes	Zhu et al., 2013	[14]
Lack of anodic capacitance	Peng et al., 2013	[15]
High substrate utilization resistance, high electron transfer resistance	Nien et al., 2011	[16]
Electron Depletion (deduced as regards of causes from previous studies, because all causes affect to production of electron)	This study	



Energy Technology, 6(2), 2017



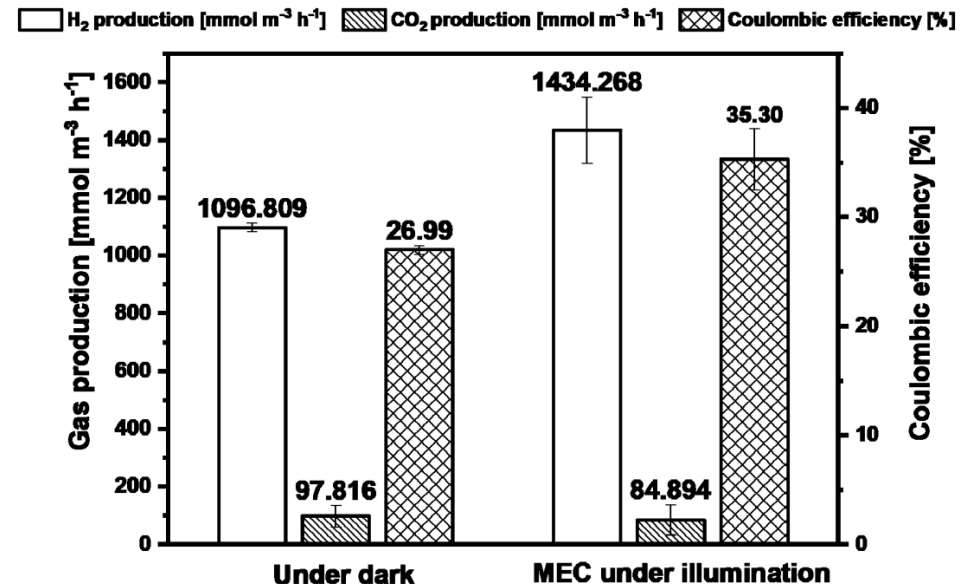
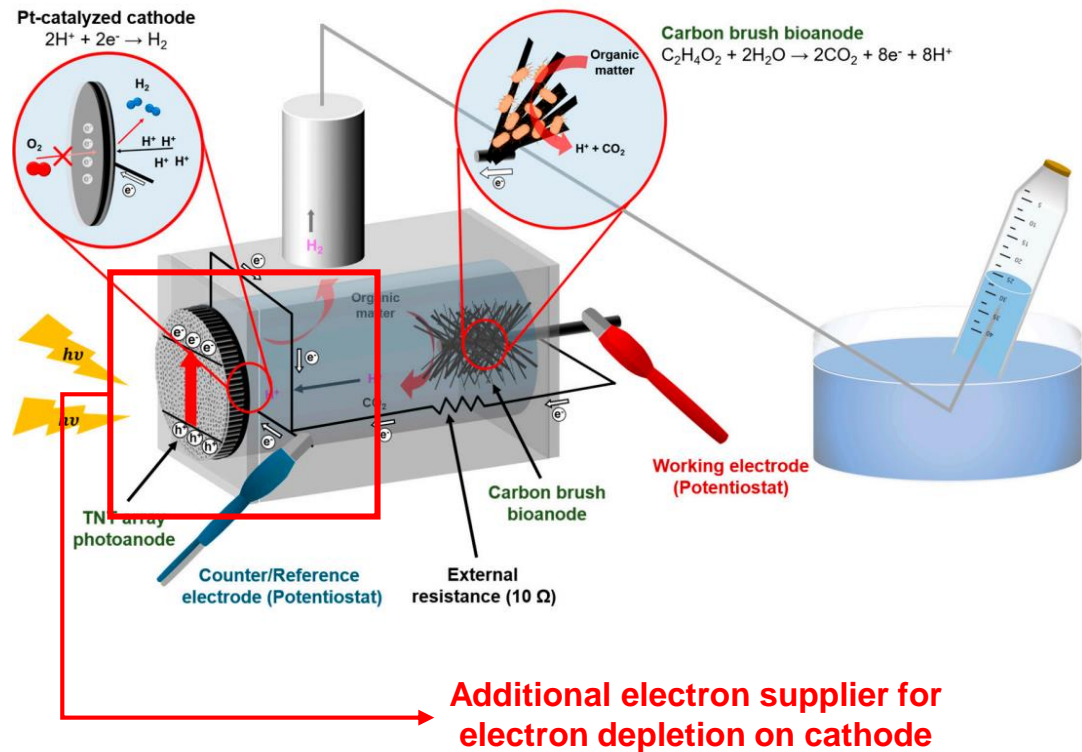


Fig 13. H₂ & CO₂ production rate, and coulombic efficiency

- MECs under dark showed a gas production rate 1096.809 mmol m⁻³ h⁻¹ H₂ and 97.816 mmol m⁻³ h⁻¹ CO₂.
- hybrid MECs showed a gas production rate 1434.268 mmol m⁻³ h⁻¹ H₂ and 84.894 mmol m⁻³ h⁻¹ CO₂. **(30.76% H₂ production rate improvement)**
- Coulombic efficiency of MECs under dark showed 26.99% and that of hybrid MECs showed 35.30%. **(8.31% improvement)**

Topic 3: C-14 Powered Dye-Sensitized Betavoltaic Cells



Chemical Communications (2020) 56, 7080-7083

Betavoltaic Cells

Technology trend

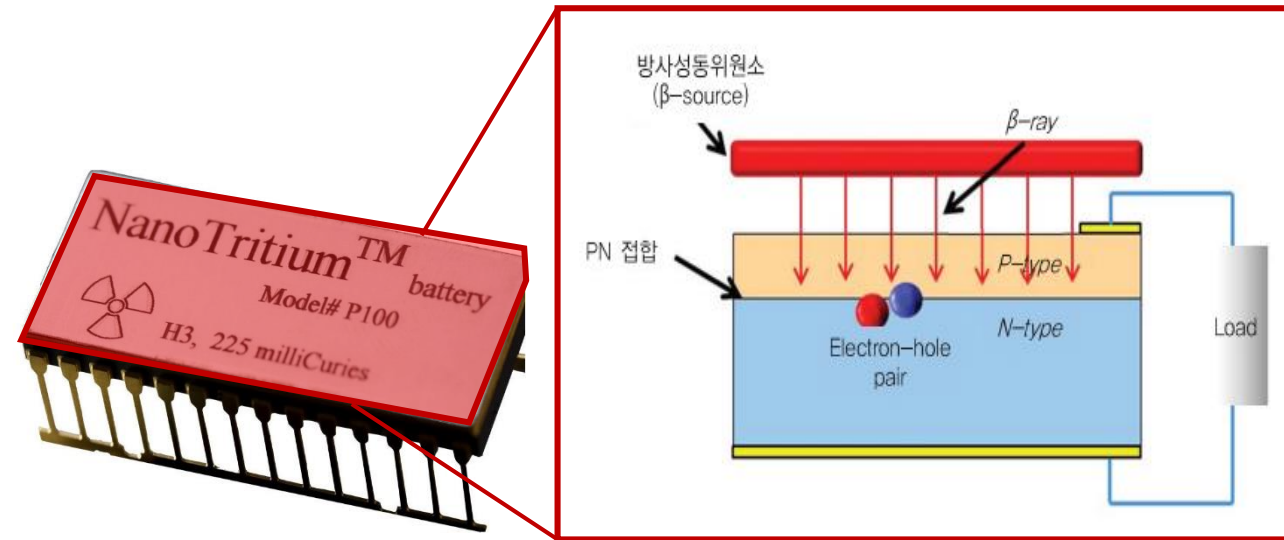


[Fig. 1] Commercialized betavoltaic battery and its operating principle.

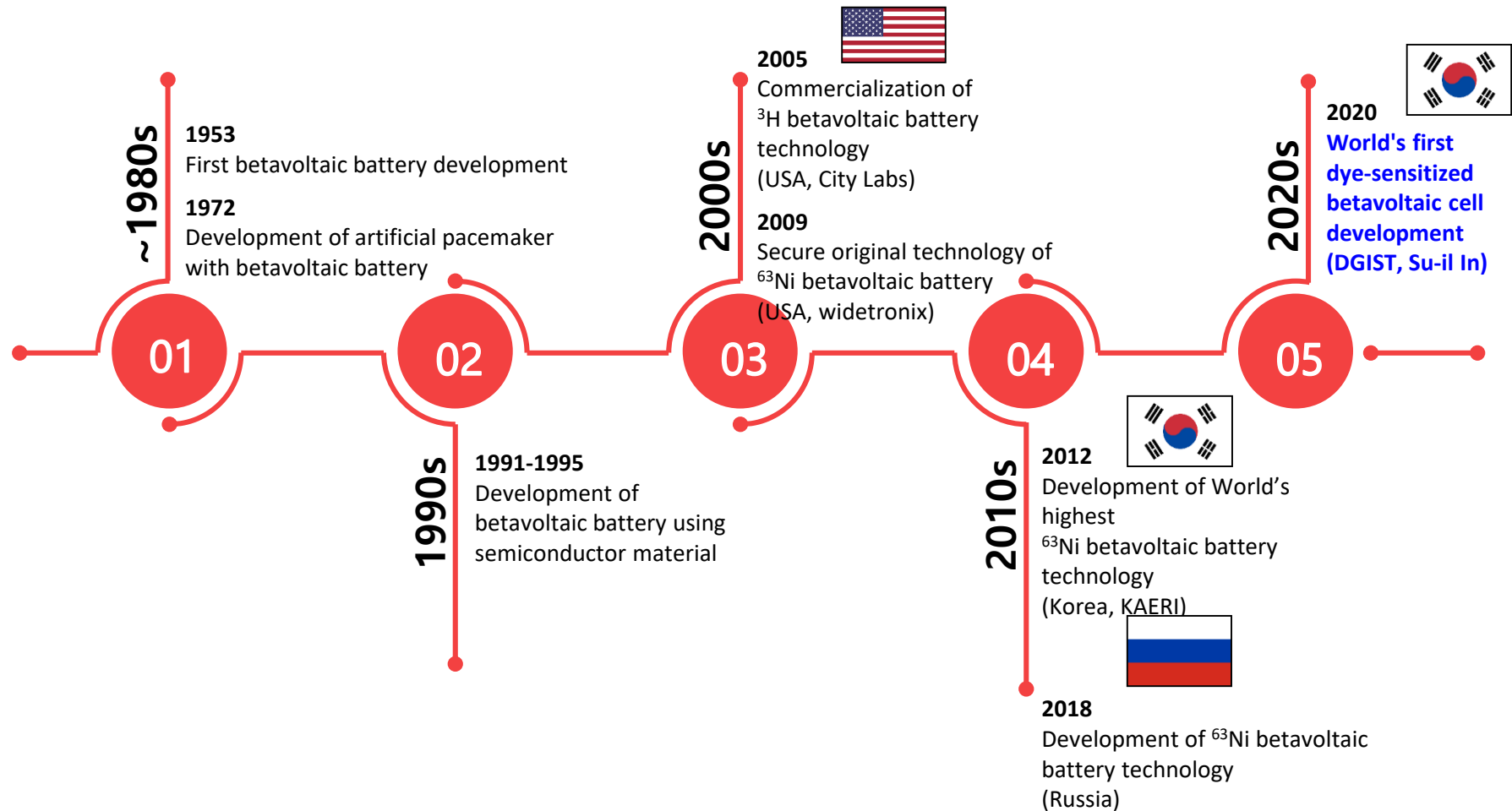
Necessity of betavoltaic battery

- With the recent development of portable devices and electric cars, the demand of long-lasting batteries increases.
- Present **lithium-ion batteries have constraints of frequent replacement, periodic charging and energy efficiency.**
- The big problem is the increasing amount of battery waste as the days go by.
- The study of the next generation of long-lived batteries is very important.
- Betavoltaic batteries are attracting a lot of attention as one of the next-generation batteries. Beta electrons from implanted radioactive isotopes collide with semiconductors and generate electricity.
- It can supply the power by its own for a long time.
(Low efficiency, complicated fabrication process and high cost are disadvantages)



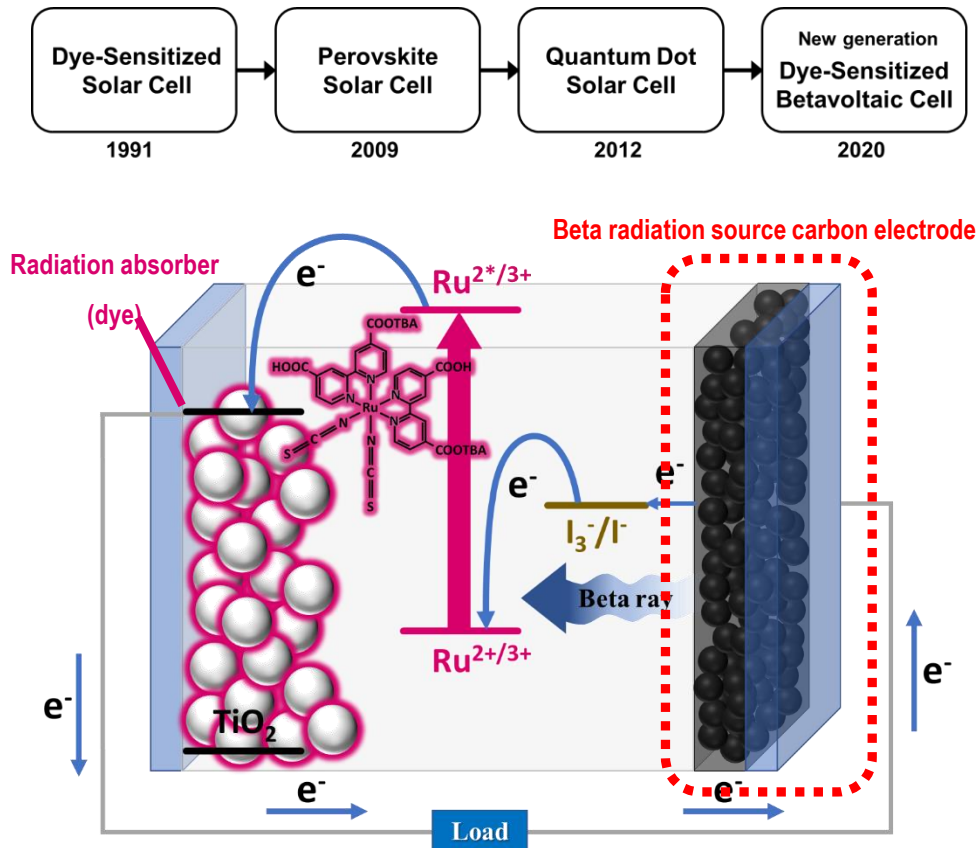
Technology trend

Betavoltaic battery technology: generation and growth



Technology concept and features

Structure and principle of betavoltaic cells using radioisotope quantum dot nanoparticles



■ Radioisotope carbon quantum dot electrode

- C-14 nanoparticles in the cathode have **dual role as counter electrode material and radioactive source** which simplify the device architecture.
- In addition, it improves performance by increasing the degree of radiation integration through C-14 nanoparticle as a beta source.

■ Radiation absorber (dye)

- There are **enhanced electron generation and transfer** by utilizing the N719 dye in the radiation absorber.
- The simple fabrication process **brings 20~30% cost savings**.

[Fig. 5] Schematic diagram of DSBC using radioisotope quantum dot nanoparticles.

Feature point of this technology

Voltage, current and efficiency analysis of betavoltaic cells using radioisotope quantum dot nanoparticles

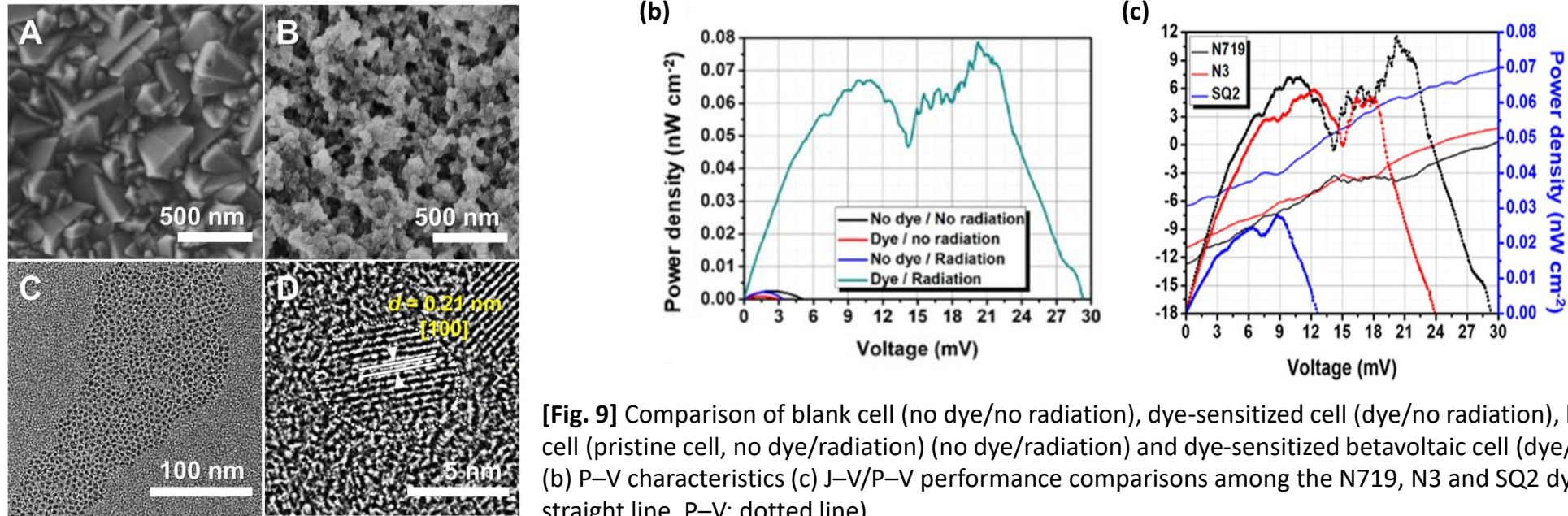


[Fig. 9] Comparison of blank cell (no dye/no radiation), dye-sensitized cell (dye/no radiation), betavoltaic cell (pristine cell, no dye/radiation) (no dye/radiation) and dye-sensitized betavoltaic cell (dye/radiation): (b) P–V characteristics (c) J–V/P–V performance comparisons among the N719, N3 and SQ2 dyes (J–V: straight line, P–V: dotted line).

- The DSBC showed an efficiency of 0.48% with the short-circuit current density (J_{sc}) 12.75 nA/cm², and the open-circuit voltage (V_{oc}) 29.2 mV.
- The DSBC generated 3.2×10^4 times more mobile electrons than those generated only by beta radiation due to the electron-impact multiple ionization or secondary ionization.
- The DSBC system using the N719 dye had a maximum power density of 0.095 nW/cm² with an energy efficiency of 0.48% because of the metal-ligand charge transition (MLCT) and difference of degrees of protonation compared to organic dye (SQ2) and N3.

Feature point of this technology

Stability test of betavoltaic cells using radioisotope quantum dot nanoparticles

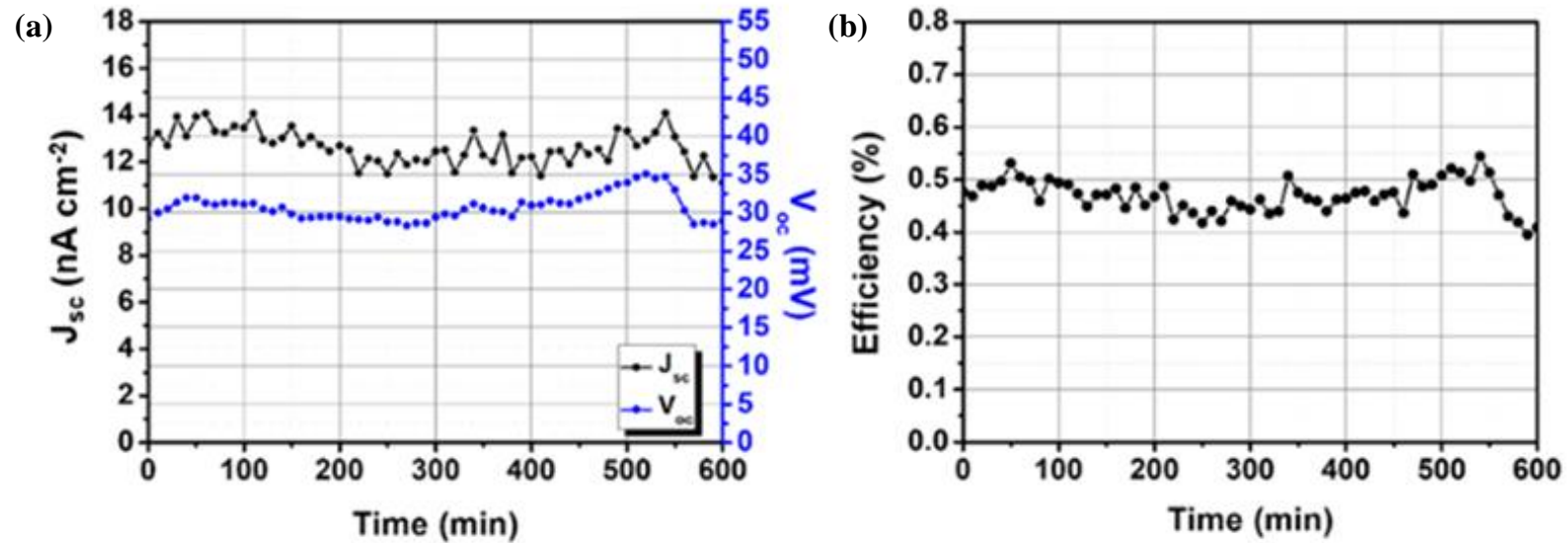
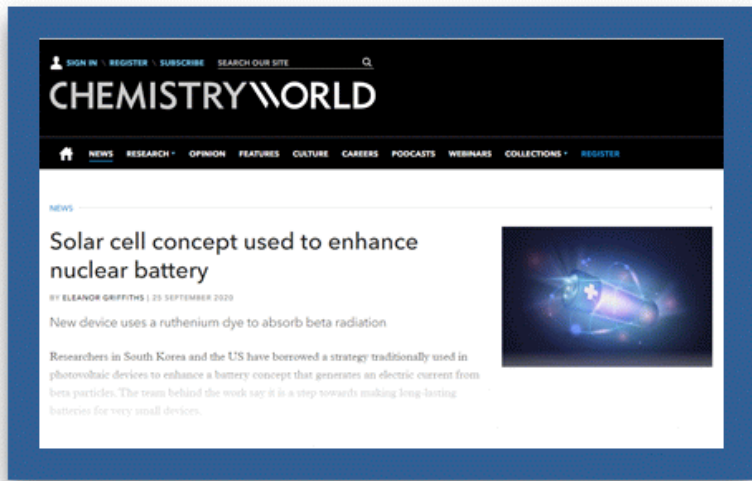


[Fig. 10] Stability of the DSBC-N719 device: (a) J_{sc} and V_{oc} and (b) efficiency.

- The stability of a DSBC-N719 over 10 hours period was measured to be 12.75 nA/cm^2 at 29.2 mV. The fluctuation in J_{sc} and V_{oc} may be due to a variable beta electron emission rate.
- The internal structure and design of the cells are suitable and stable.



충전 없이 평생 쓰는 배터리 나온다



대구=정재훈기자
jhoon@etnews.com

대학 연구팀이 별도 충전 없이 반영구적으로 사용 가능한 염료감응 베타전지를 개발했다. 극한 환경이나 의료 분야 차세대 전원으로 활용될 수 있을 것으로 기대된다.

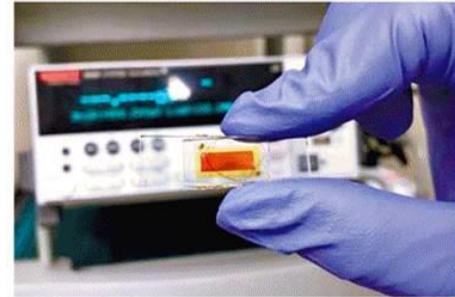
대구경북과학기술원(DGIST·총장 국양)은 인수일 에너지공학전공 교수팀이 베타선에 염료가 반응하는 원리를 응용해 값싸고 안전한 반영구 베타전지를 최초로 개발했다고 15일 밝혔다.

기존 전지는 우주, 심해 등 극한 환경에서 사용하기에 전력과 장기 안정성이 떨어지고, 수명도 짧다. 게다가 잦은 교체 주기에 따른 폐기물 발생으로 환경 문제를 일으킨다.

베타전지는 방사성 동위원소를 원료로 이용하는 차세대 전지 중 하나다. 방사성 동위원소에서 방출된 베타전자가 방사선흡수체인 반도체에 충돌하면서 전기를 생산하는 원리다.

베타선은 인체 유해성과 투과도가 낮아 높은 안전성을 띤다. 외부 동력원 없이 자체 전력 생산이 가능해 별도의 충전이 필요 없다. 수명은 방사성 동위원소의 반감기와 비례하기 때문에 교체 주기가 길다. 미국과 러시아 등 세계 주요

DGIST, 염료감응 베타전지 개발
동위원소 '탄소-14'로 구조 단순화
반감기 5730년...반영구 사용 가능
우주·의료 분야 차세대 전원 기대



인수일 DGIST 교수팀이 개발한 염료감응 베타전지.

국가가 베타전자 연구에 각축을 벌이고 있는 이유다. 하지만 소재가 비싸고 복잡한 제작 공정 때문에 대량생산이 쉽지 않다.

인 교수팀은 기존 베타전지에서 방사선흡수체로 사용된 값비싼 반도체 물질을 '루테늄(Ruthenium:주기율표의 중앙에 위치하는 전이금속으로, 백금족 금속의 하나)' 계열의 'N719'

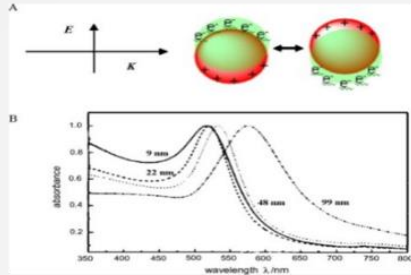
염료로 대체했다. 또 베타선을 방출하는 동위원소 '탄소-14'를 적용해 기존 베타전지가 가진 복잡한 구조를 단순화했다. 탄소-14를 나노입자로 만들어 에너지 밀도를 높였다. 염료감응 베타전지 성능실험을 통해 탄소-14에서 방출된 전자 대비 3만2000배의 전자를 생성하며 10시간 동안 안정적으로 전력을 생산한다는 것을 관찰했다. 특히 베타전지에 사용된 탄소-14는 약 5730년의 반감기를 가지고 있어 상용화에 성공하면 반영구적 수명을 가질 것으로 예상된다.

이번 연구는 베타전지분야에서 새로운 구조와 방사선 흡수체에 적용할 수 있는 물질의 다양성을 제시했다는데 의미가 있다. 연구팀은 후속연구로 베타전지 효율을 실용화 수준까지 끌어올릴 계획이다. 실용화에 성공하면 우주와 심해 등 극한 환경뿐 아니라 의료분야 차세대 전원으로도 활용 가능하다.

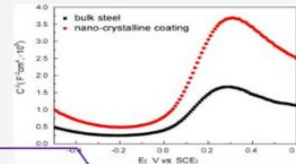
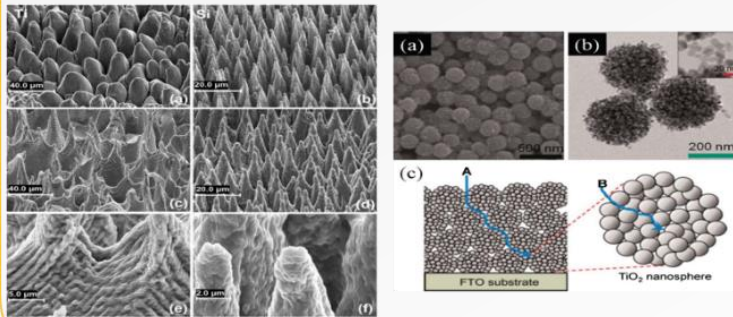
인수일 교수는 "값싼 염료를 적용, 새로운 베타전지 개발에 성공했다는데 의미가 있다"면서 "아직 풀어야 할 숙제가 많지만 안전하고 저렴한 염료감응 베타전지 개발에 노력하겠다"고 밝혔다. 인 교수는 2010년부터 2년 동안 미국 펜실베이니아주립대 화학과, 재료공학과 박사 후 연구원으로 활동한 뒤 DGIST 에너지공학전공 교수로 부임해 차세대 에너지 분야를 집중 연구하고 있다.

Topic 4: Nano-Bio Hybrid Science and Technology

Plasmonic Effect

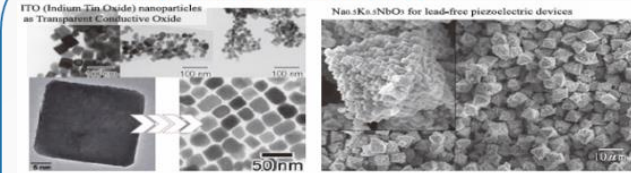


Variety Structure Fabrication

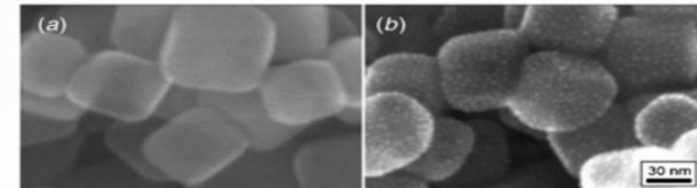
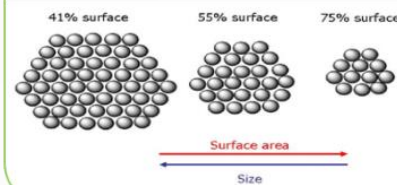


Size Effect – Signal Change

Hybrid NP & Alloy



Surface Area



Drug misuse/overdose and environmental pollution

Pain Killer Overdose

Deaths from drug overdose have been rising steadily over the past two decades and have become the leading cause of injury death in the United States.



Nearly **9 out of 10** poisoning deaths are caused by drugs.

Drug overdose death rates have been rising steadily since 1992 with a **102% increase** from 1999 to 2010 alone.

Every day in the United States, **105 people die** as a result of drug overdose.

6,497 (30%) Benzodiazepines.

16,651 (75%) Opioid Analgesics

Of the **22,134 deaths** relating to prescription drug overdose in 2010, **16,651 (75%)** involved opioid analgesics (also called opioid pain relievers or prescription painkillers), and **6,497 (30%)** involved benzodiazepines.

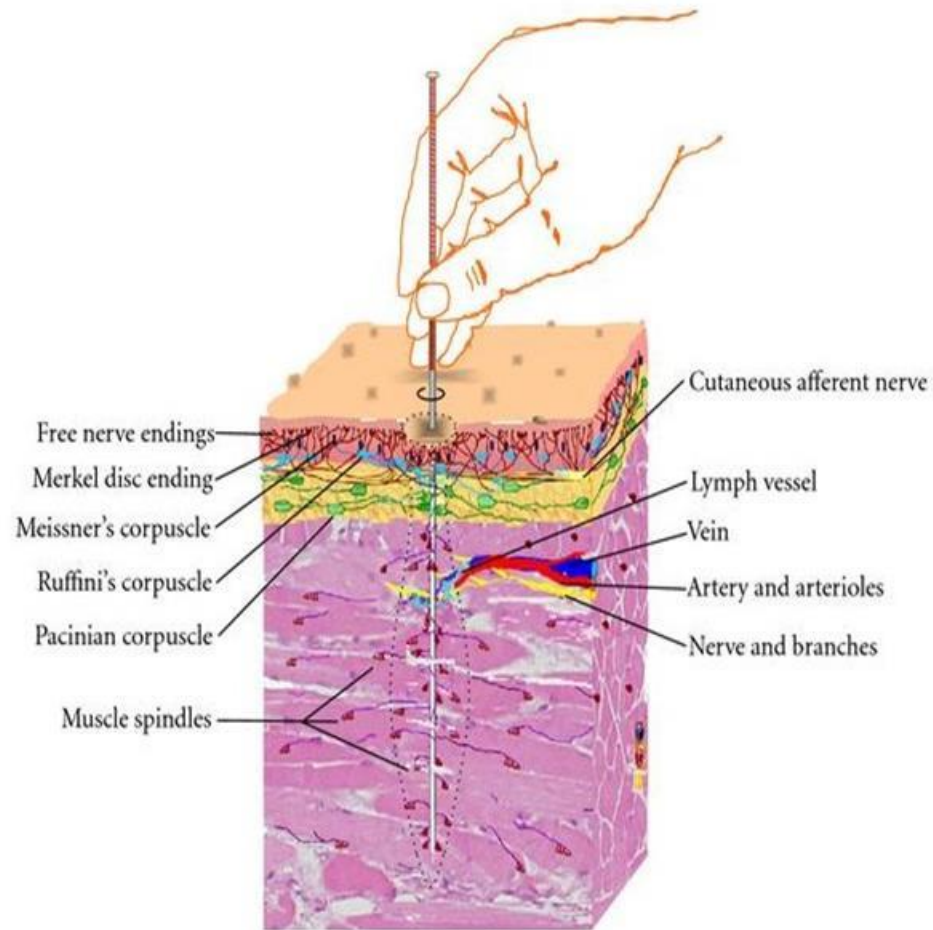
Source: <http://www.cdc.gov/homeandcommunityhealth/halt/prevention/overdose-facts.html>

It's **NOT TOO LATE** for **HELP**
Visit OnlineDrugClass.com to see what we can do to help get your life back on track.



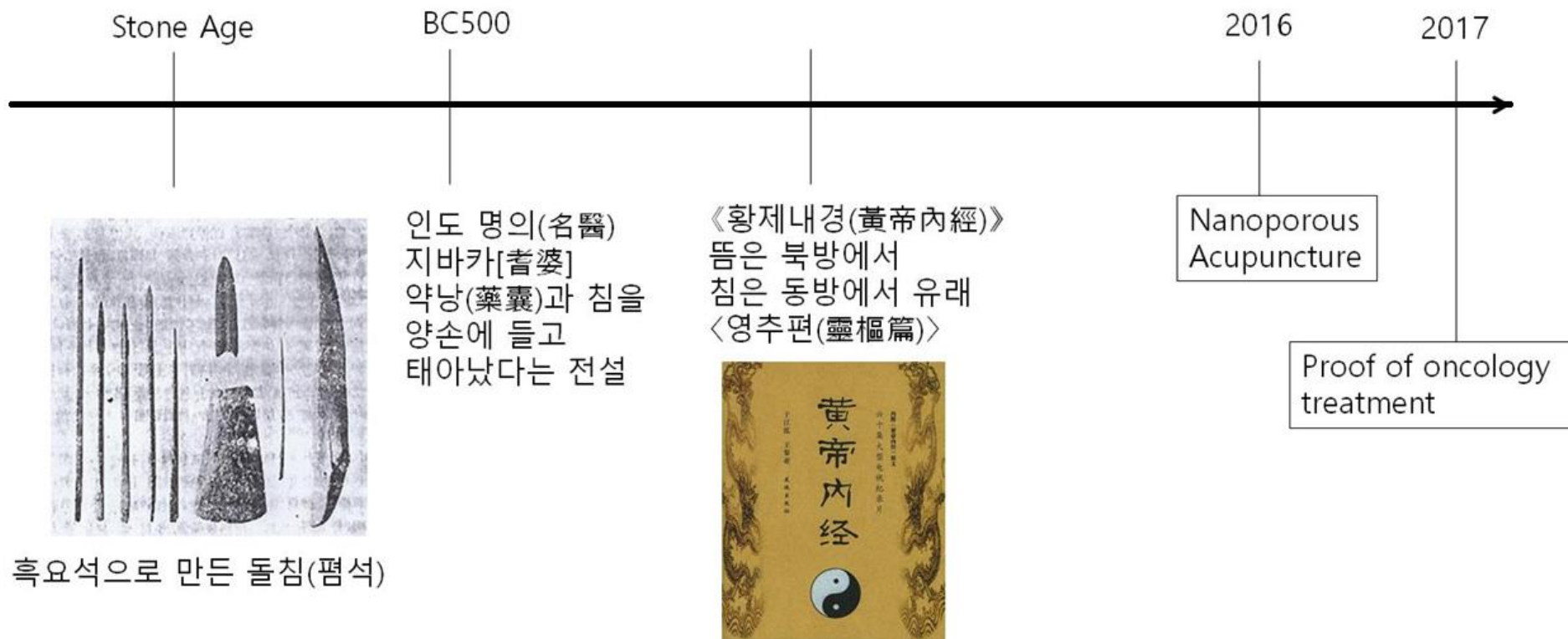
Introduction

Acupuncture therapy



- The invention of acupuncture as a therapeutic treatment is traced as far back as 6000 B.C., originating with the insertion of sharpened stones at specific acupuncture points.
- An acupuncture device is made by metal acupuncture needles, including those of gold, silver, copper, and stainless steel.
- We hypothesize that an increase in needle surface area with no significant variation in needle diameter may lead to increased interactions of surrounding tissue, leading to enhanced acupuncture stimuli. -> autoimmune system

Brief History of Acupuncture



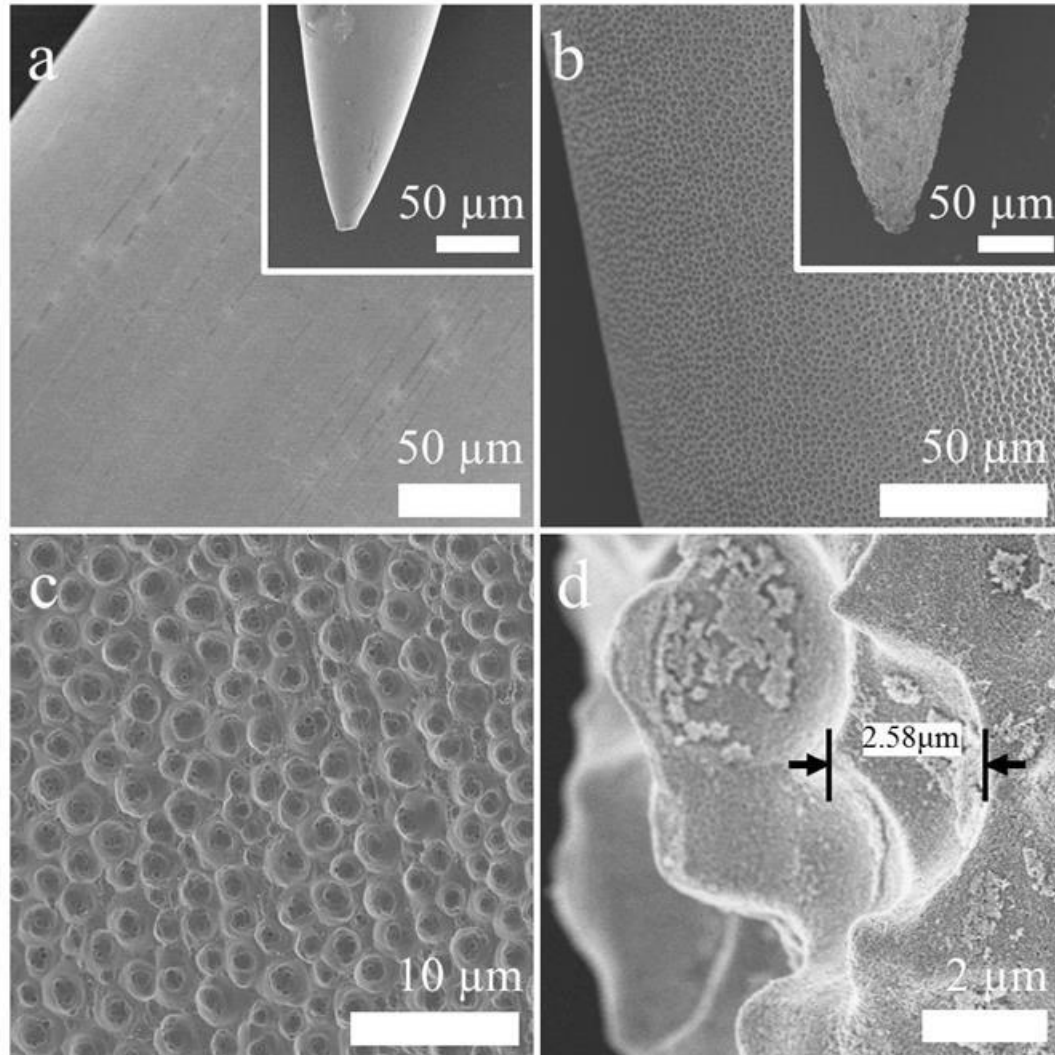
Hierarchical Micro/Nano-Porous Acupuncture Needles Offering Enhanced Therapeutic Properties

Scientific Reports 2016, 6, 34061

Enhanced Therapeutic Treatment of Colorectal Cancer Using Surface-Modified Nanoporous Acupuncture Needles

Scientific Reports 7 (2017) 12900

- SEM (Scanning Electron Microscope)

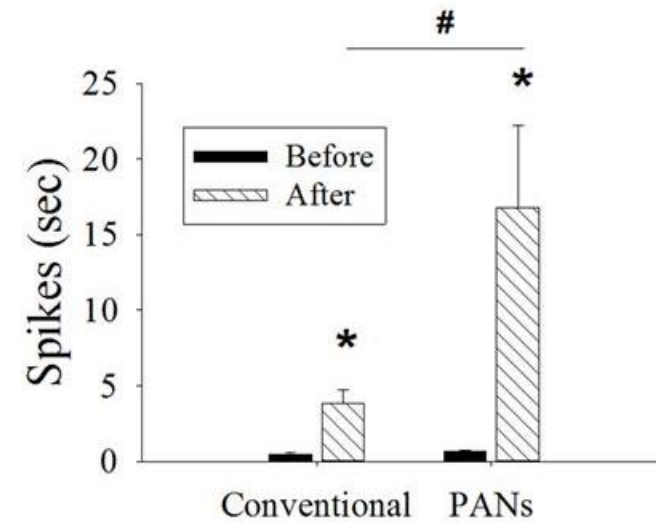
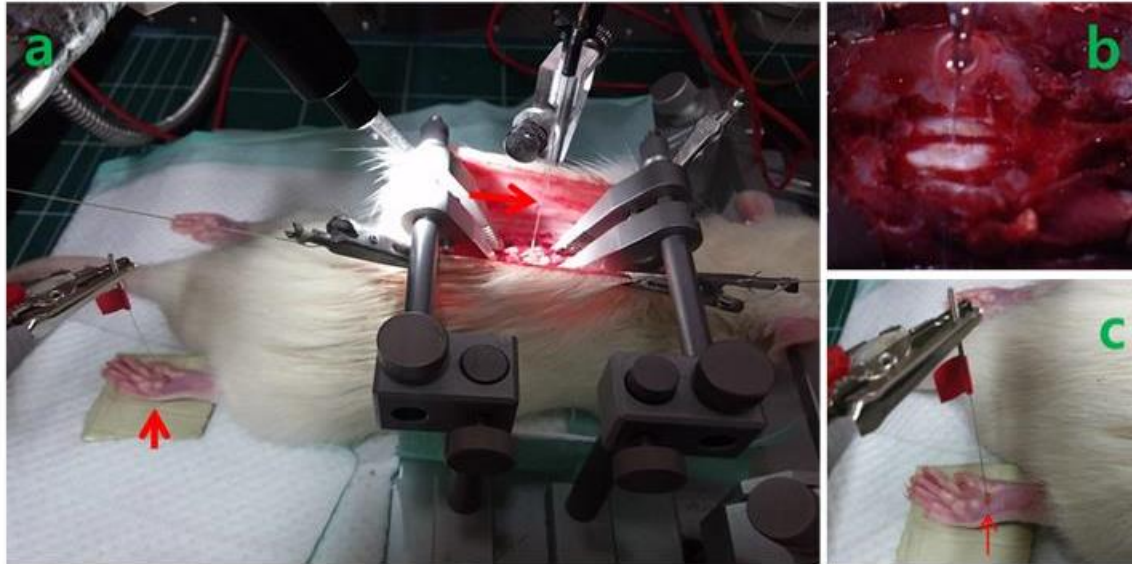


- (a) Conventional stainless steel needle
- (b) Porous anodized needle
- (c) Enlarged image of (b)
- (d) Cross-sectional image of the porous anodized needle.

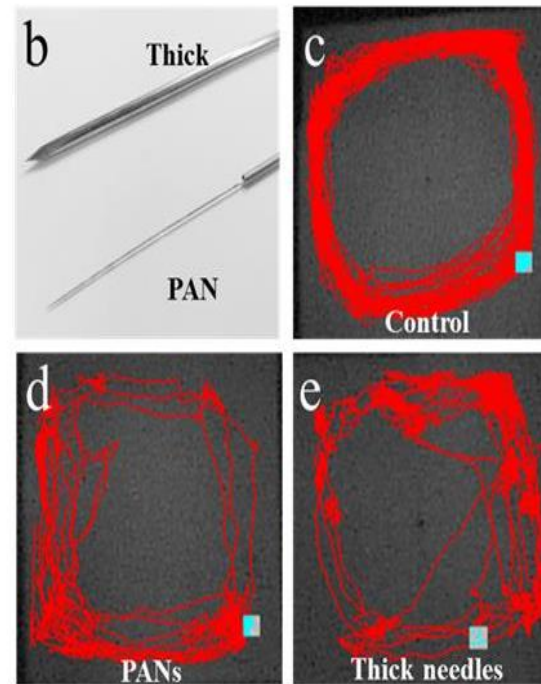
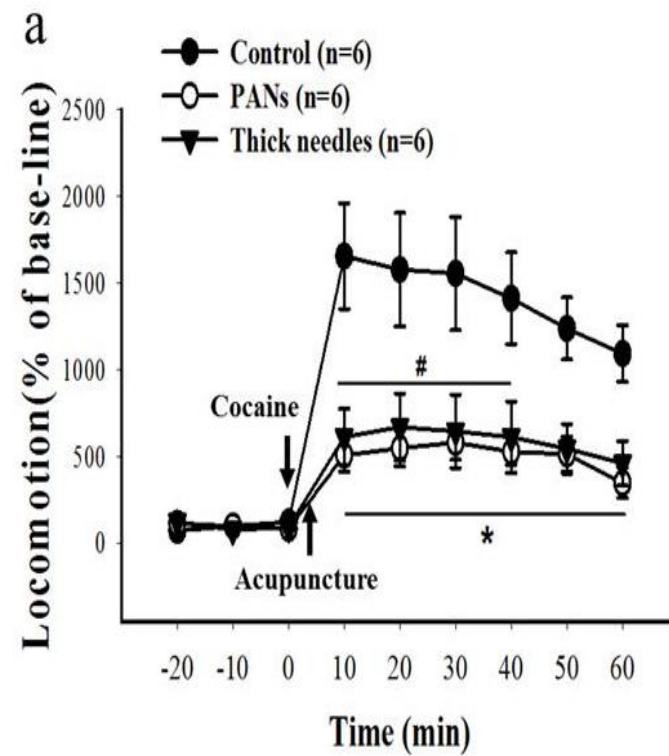
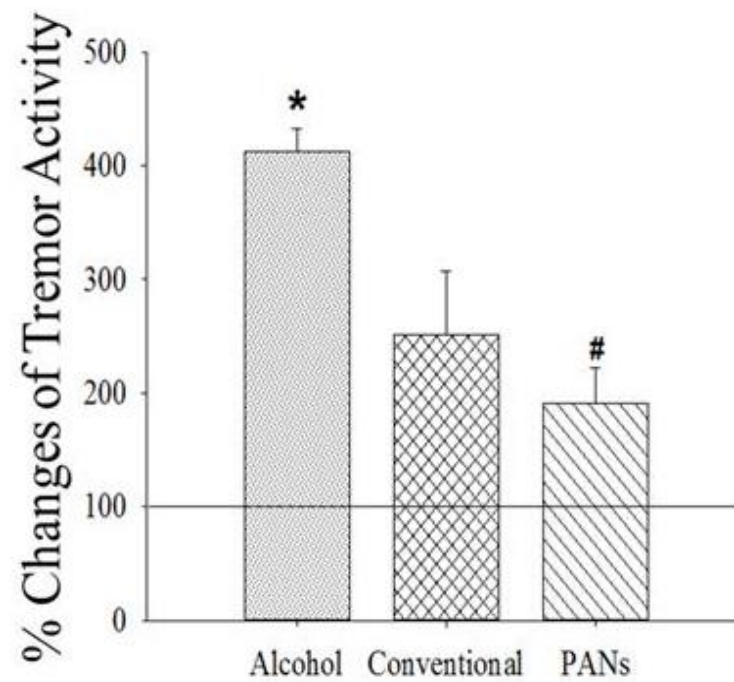
Insets of (a, b) show needle tips.

- One can see that the pores are conical in shape, tapering in size from 3.0 μ m at the surface to 0.05 μ m, with a cone depth varying from 1.0 to 2.6 μ m.
- No formation or loss of any element in the acupuncture needle is detected, assuring that electrochemical anodization doesn't change the chemistry of the acupuncture needle.

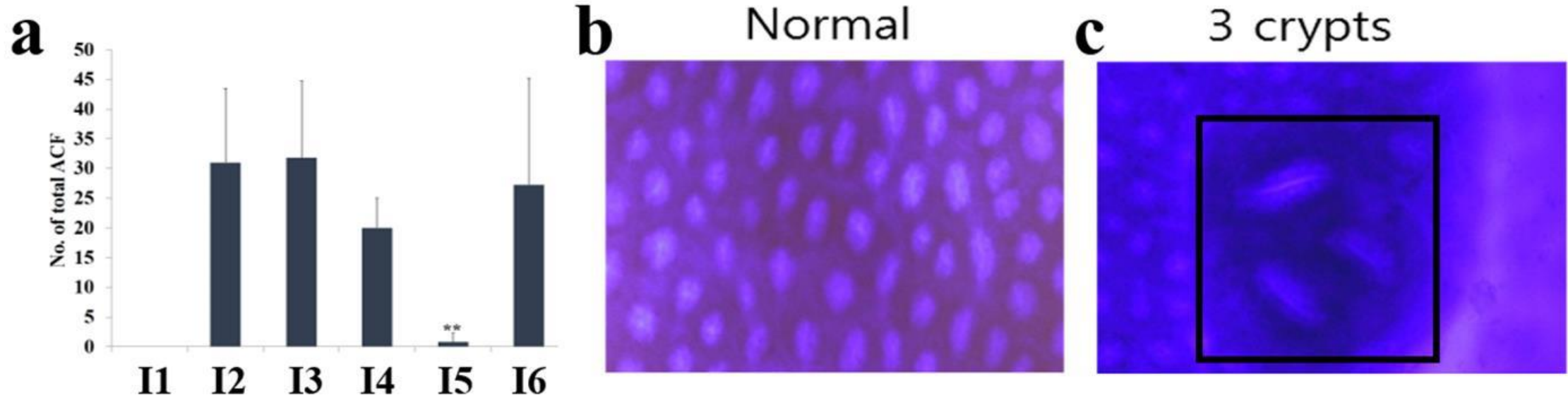
II. Neuronal activity



Conventional and PAN groups show increased neuronal activity to needle stimulation (after) compared to before stimulation (* $p < 0.05$). In addition, PAN group shows a significant increase in stimulation-induced neuronal activity compared to conventional group (# $p < 0.05$).



- Early stage colorectal cancer (CRC) gene expression analysis and aberrant crypt foci (ACF) formation



- ACF increase in crypt multiplicity with time, and thus are accepted as a predictor of tumor progression
- The mean number of total ACF in I2 was 31.0 ± 12.5
- The ACF count dramatically decreased to 0.8 ± 1.5 ACF/colon in I5, demonstrating that PN at HT7 acupuncture significantly inhibits AOM-induced colonic AC formation
- The reduced ACF number is, presumably, closely related to the recovered expression of genes altered by AOM exposure.

Average number of ACF found in each group. The experimental conditions of initiation groups I2-I6, all at early stage CRC, are as follow: I2 = positive control(AOM injection only); I3 = CN acupuncture treatment at HT7 point; I4 = CN acupuncture treatment at SI5 point; I5 = PN acupuncture treatment at HT7 point; and I6 = PN acupuncture treatment at SI5 point.

- Analysis of tumor size and cancer biomarker (CEA)

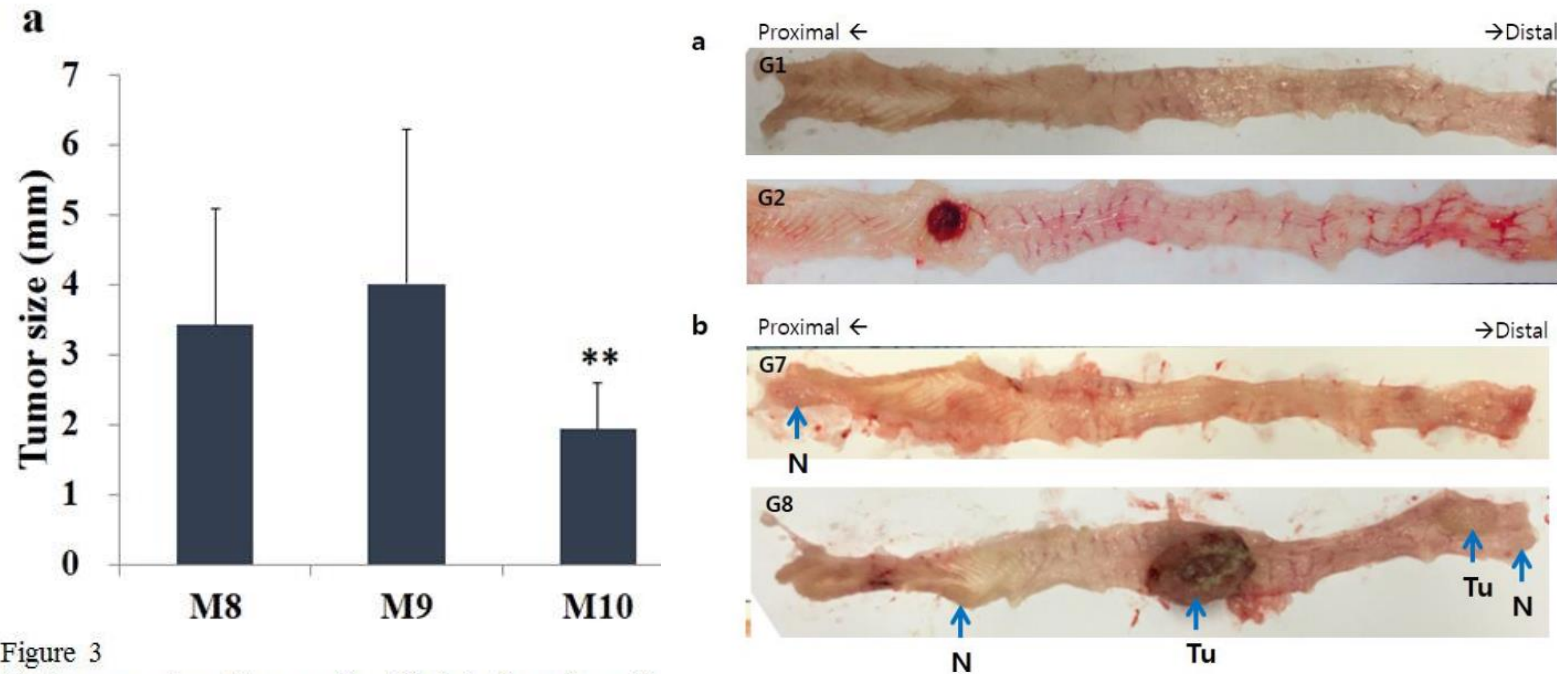


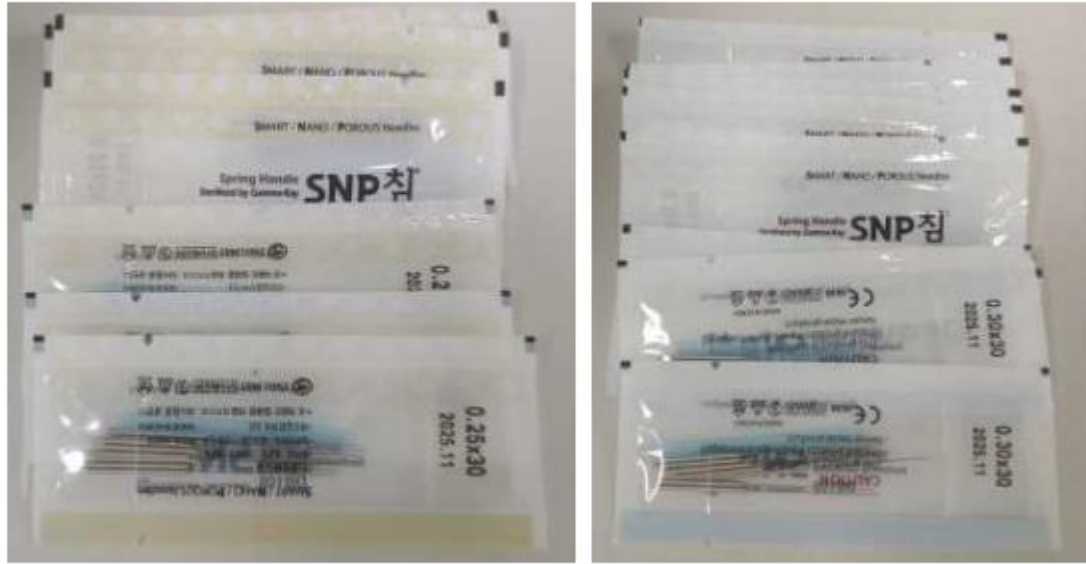
Figure 3

(a) Average size of tumors identified in the colon of animals from each experimental group.

(b) Expression of the circulating colorectal cancer biomarker, CEA. All animals were treated by acupuncture at acupoint HT7 every day for 40 weeks after the last azoxymethane (AOM) injection. M8, positive control; M9, treated with the conventional needle (CN); M10, treated with the nano-porous needle (PN). Maturation groups M7-M10, all at late stage CRC, have experimental conditions: M7 = negative control (no treatment); M8 = Positive control (AOM injection only); M9 = CN acupuncture treatment at HT7 point; and M10 = PN acupuncture treatment at HT7 point.

- The average tumor size observed in M10 was significantly decreased from that of M8
- Figure 3b shows a significant decrease in the average CEA concentration in M9 and M10 compared to M8, providing further evidence as to the efficacy of acupuncture treatment

[제품개발] Smart Nano Porous Needles (SNP Needles, SNP침) 시제품 이미지



[첨부1_그림1] 국문(좌) 영문(우) 씬지에 포장된 시제품 SNP침 모습



[첨부1_그림2] 국문(좌) 영문(우) 박스에 포장된 시제품 SNP침 모습



8. Acknowledgement



Prof. Michael Hoffmann

Prof. Tetsuro Majima

Prof. James Durrant

Prof. Abdul Razaq

Dr. Saurav Sorcar

- Ph.D candidate

Hyerim Kim

Young-ho Park

Yunju Hwang

Ali Shahzad

Hong-Soo Kim

Chaitanya Hiragond

Hwapyong Kim

- M.S. candidate

Eunhee Gong

Junho Lee

Dongyun Kim

Flores Monica Claire

- Contributors of alumnis

Dr. Abdul Razzaq

Sunghyun Lee

Kinam Kim

Funding

This research was supported by a grant of the Korean National Research Foundation

Thank you!

Q&A